Arch. Mech., **55**, 1, pp. 3–38, Warszawa 2003

# Modelling adiabatic shear banding via damage mechanics approach

P. LONGERE[(1)], A. DRAGON[(1)], H. TRUMEL[(1)],
T. DE RESSEGUIER[(2)], X. DEPRINCE[(3)] and E. PETITPAS[(3)]

[(1)] *Laboratoire de Mécanique et de Physique des Matériaux, UMR CNRS n° 6617 – ENSMA 1 avenue C. Ader, BP 40109, 86962 FUTUROSCOPE- CHASSENEUIL Cedex, France*

[(2)] *Laboratoire de Combustion et de Détonique, UPR CNRS n° 9028 – ENSMA 1 avenue C. Ader, BP 40109, 86962 FUTUROSCOPE-CHASSENEUIL Cedex, France*

[(3)] *Centre de Recherches et d'Etudes Technologiques – GIAT Industries 7 route de Guerry, 18023 BOURGES Cedex, France*

*Dedicated to Professor Piotr Perzyna on the occasion of his $70^{th}$ birthday*

DURING DYNAMIC LOADING PROCESSES, large plastic deformation associated with high strain rates leads, for a broad class of ductile metals, to degradation and failure by adiabatic shear banding. The paper presents an attempt to model some salient features of this process viewed as an anisotropic damage mechanism coupled with thermo-elastic/viscoplastic deformation. The model is destined to be applied in the context of high velocity impact and penetration mechanics. The methodology employed within the framework of the internal state variable structure strives to keep a middle way between extensive description of complex viscoplastic flow and damage events and application-oriented accessibility requirements. Model capabilities are prelaminarily illustrated for shear loading process.

## 1. Introduction and scope

DYNAMIC LOADING CONDITIONS such like high-velocity impact and penetration (see Figs. 1, 2), explosive vs. metal interaction, high-speed machining and other, imply high strain-rate viscoplastic flow characterized by negligible redistribution of the heat generated by plastic deformation. The process is essentially adiabatic and leads to thermal softening which, at some advanced stage of deformation, becomes prevailing against the strain and strain-rate hardening. One observes a decrease in the flow stress and large plastic strain localization within narrow regions known as adiabatic shear bands. The latter are most frequently

observed in high-strength alloys and steels (see e.g. WOODWARD [1] and NEMAT-NASSER *et al.* [2]). A significant temperature difference exists between the inside of bands and the outside. Adiabatic shear band localization phenomena are generally attributed to plastic instability events generated by thermal softening, see e.g. BAI [3] and WRIGHT and BATRA [4]. Extensive investigation and literature have been devoted to the matter in the 1980's and later. The experimental studies by MARCHAND and DUFFY [5], employing thin-walled tubes twisted at high strain rates by means of a torsional KOLSKY bar set-up, are most frequently cited. The reader can find more references, including the earliest investigations into the fracturing by adiabatic shear banding from the mid of the $20^{\text{th}}$ century on, in WOODWARD [1]. As stated by MERCIER and MOLINARI [6], most of the early theoretical approaches to the subject considered a shear band as a one-dimensional entity in a much simplified context of material behaviour. A great number of studies in the 1990's went deeper into multiform material parameter influence on multiple shear band forming, spacing, characteristic thickness and related propagation phenomena (velocity, extension of the process zone), see e.g. MOLINARI [7] and GRADY [8]. Most of those analyses are performed by zooming on an elementary layer under simple shear loading conditions. Various approaches of instability have been advanced and connected with the geometric pattern of shear bands, e.g. MOLINARI [7] and PĘCHERSKI [9].

PERZYNA was probably the first to have incorporated the shear band formation into three-dimensional (3D) modelling, regarding viscoplastic flow coupled with micro-damage process embodied by specific internal variable(s). In the paper [10] adiabatic shear band localization under dynamic loading conditions has been considered together with spalling by ductile void formation in the modelling framework insisting on and turned towards induced anisotropic effects. The microdamage mechanism by nucleation and growth of microcracks is dealt with in [10]. The anisotropic nature of the process is accounted for by specific hypotheses concerning the distribution and the shape of defects including a random nature of micro-damage evolution. The more recent papers by ŁODYGOWSKI and PERZYNA [11] and DORNOWSKI and PERZYNA [12] focus even more on fracturing phenomena related to localized adiabatic shearing in a quantitatively elaborated damage modelling coupled with thermo-viscoplastic flow. The well-posedness of the evolution problem and numerical regularization aspects are discussed in the framework of consistent formulation of the discretized initial-boundary-value problem.

The objectives of the present paper are clearly situated in the above perspective traced by PERZYNA's damage-and-viscoplasticity 3D modelling of ductile metals at large strains and high strain rates. Including specific anisotropy effects induced by a particular deterioration mechanism, i.e. shear banding related damage, it is being done in an alternative manner based on the second

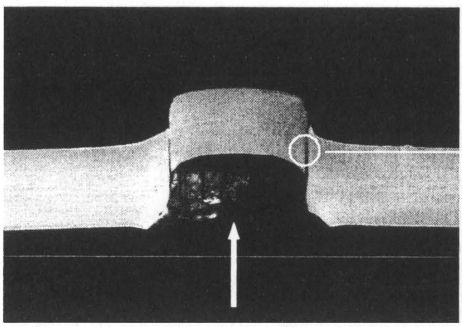

FIG. 1. Impacted hard steel plate (after GIAT Industries).

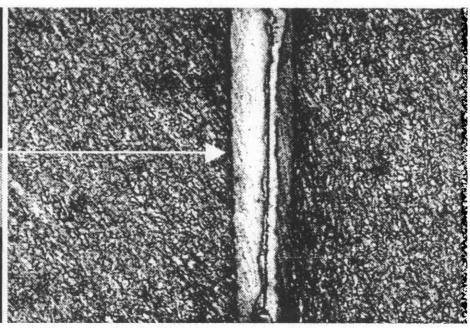

FIG. 2. Adiabatic shear band with ultimate crack (after GIAT Industries).

authors earlier contributions to anisotropic damage, see e.g. the synthetic review by DRAGON *et al.* [13]. The highly non-trivial and still arduous problem of combining finite-strain plasticity and anisotropy effects is being considered here using Mandel-Sidoroff framework, see e.g. MANDEL [14] and SIDOROFF and DOGUI [15].

The present work presents an attempt to model some salient features of damage by shear banding as coupled with thermo-elastic/viscoplastic deformation, involving multifold anisotropy effects while introducing some simplifying hypotheses (e.g. as concerns plastic hardening). The purpose is to get a tractable model to be applied in the context of high-velocity impact and penetration mechanics.

The paper is organized as follows: in Sec. 2 preliminary remarks concerning internal damage variable related to adiabatic shear bands (ASB) are given and some terminology is introduced. In Sec. 3 large deformation thermo-elastic/viscoplastic model with internal variables and damage-induced anisotropy effects is introduced and discussed. An auxiliary analysis, allowing for evaluation of the onset of instability via thermo-viscoplastic perturbation method, is employed to pose a damage-inception criterion. This analysis is summarized in Sec. 4. In Sec. 5 the constitutive model is preliminarily but extensively tested on a homogeneous volume element (material point) under simple shear loading. Some comments concerning the identification and bounding of material parameters are also given in Sec. 5.

## 2. The ASB-related damage variable and kinematic preliminaries

In this paper, we are interested in the description of the material behaviour in the presence of ASB considered as damage mechanism to be put forward in the framework of a 3D continuous model: within this model, the deterioration

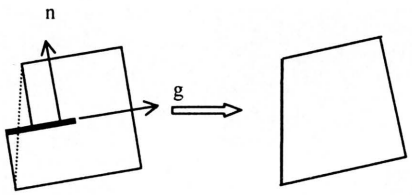


FIG. 3. Equivalent homogeneous volume element ($\alpha = 1$).

at stake is to be captured by a corresponding internal variable, its evolution and its effect on elastic stiffness and viscoplastic flow. The model should be robust enough to overcome local instabilities relative to inception and growth of ASB on mesoscale level. Another feature to be accounted for by this model is a strongly oriented character of ASB, thus inducing significant mechanical anisotropy with both elasticity and plasticity being potentially affected.

In order to describe the anisotropic degradation state of the material caused by the presence of ASB, a 2nd order tensorial damage variable is introduced. Its components are denoted as $D_{ij}$ and are expressed by (2.1), where $d^\alpha$ and $\mathbf{n}^\alpha$ represent respectively the scalar intensity and the orientation of the band pattern $\alpha$ (see Fig. 3).

$$
\begin{aligned}
D_{ij} &= \sum_\alpha d^\alpha \cdot N_{ij}^\alpha , \\
N_{ij}^\alpha &= n_i^\alpha n_j^\alpha .
\end{aligned}
\tag{2.1}
$$

As discussed before, the onset and further evolution of adiabatic shear banding are a consequence of thermal softening, respectively in the sound material during locally homogeneous plastic deformation, and inside the bands themselves during evolving localization process. The intensity $d^\alpha$ includes consequently information relative to temperature inside the band pattern $\alpha$. Consider now a single band pattern ($\alpha = 1$), and introduce the adjective "singular" for the processes relevant strictly to the adiabatic shear banding, and the adjective "regular" for the processes not relevant to the adiabatic shear banding. With such a distinction, the current density $d$ of the damage variable $\mathbf{D}$ depends on "singular" temperature, and can thus be written as:

$$
d = d(T^*, ...) \tag{2.2}
$$

where $T^*$ represents the "singular" temperature, and where the dots represent other possible arguments.

The lower bound $d_{\min} = d(T_0^*, ...)$ of the density $d$ is obviously zero, $T_0^*$ representing the initial "singular" temperature value which is equal to the "regular"

temperature value at the incipience of damage. On the other hand, temperature is supposed to be bounded in the band material by the melting point. This is probably a strongly over-estimating statement (see e.g. [1]) for metallic materials subject to this mechanism of adiabatic shear banding. The density $d$ of the damage variable $\mathbf{D}$ is consequently bounded too. The upper bound of $d$ is denoted by $d_{\max} = d(T_m, ...)$, where $T_m$ represents the temperature value at the melting point. In Sec. 5, an estimation of $d_{\max}$ is given based on mechanical considerations for the case of simple shear.

The geometric consequences of the shear band pattern (Fig. 3) are viewed as those of a "super-dislocation" (see also PĘCHERSKI [9]). By using concepts of the crystalline plasticity, the damage-induced supplementary strain rate $\mathbf{d^d}$ is introduced as the result of the glide velocity $\dot{\gamma}^\alpha$ caused by the band pattern $\alpha$ of normal $\mathbf{n^\alpha}$ and with orientation $\mathbf{g^\alpha}$ (see Fig. 3):

$$
\begin{aligned}
d^d_{ij} &\propto \sum_\alpha \dot{\gamma}^\alpha M^\alpha_{ij}, \\
M^\alpha_{ij} &= \left(g^\alpha_i n^\alpha_j\right)^S = \frac{1}{2}\left(g^\alpha_i n^\alpha_j + g^\alpha_j n^\alpha_i\right).
\end{aligned}
\tag{2.3}
$$

The kinematic variable $\mathbf{d^d}$ allows to smooth the boundary discontinuity caused by the ASB (see Fig. 3). There are thus two contributions to the inelastic evolution of the equivalent homogeneous volume element: the "regular" plastic strain rate, denoted by $\mathbf{d^p}$, and the "singular" damage induced strain rate, denoted by $\mathbf{d^d}$. The total inelastic strain rate $\mathbf{d^{dp}}$ is written as the sum of those two contributions:

$$
d^{dp}_{ij} = d^p_{ij} + d^d_{ij}\,. \tag{2.4}
$$

Further on, care must be taken to ensure the concomitance of the two rates $\overset{\mathbf{0}}{\mathbf{D}}$ (an objective derivative of $\mathbf{D}$ to be defined) and $\mathbf{d^d}$, which are both relative to the same process of ASB-induced damage.

On the other hand, very large strains and rotations occurring during the adiabatic shear banding process make the finite elastic-plastic deformation framework indispensable. Since pioneer MANDEL's works [14], many valuable contributions appeared concerning the introduction of (initial and/or induced) anisotropy in the context of large elastic-plastic strains. Despite this, the problem remains still open, see e.g. SIDOROFF and DOGUI [15] and EKH and RUNESSON [16]. In the present approach, a spatial vision of the motion is adopted in order to preserve the physical signification of the state variables, of their derivatives and of their conjugate forces. Clearly, the Eulerian point of view is suitable to deal with plasticity whose rheology is close to the fluid one in some aspects [15]. However, the Eulerian point of view is not proper to identify material symmetries. In isotropic

elastic-plastic media, the rotation required to define the intermediate configuration is in fact of secondary importance, and rotational and material derivatives lead to the objectivity of the incremental constitutive model as well. With regard to anisotropic elastic-plastic media, the definition of the rotation becomes essential [14].

## 3. Large deformation damage-viscoplasticity constitutive model with ASB-anisotropy effects

The constitutive model to be formulated must be able to describe the thermo-elastic/viscoplastic behaviour of the sound material and the mechanical anisotropy (directional degradation of both the elastic and viscoplastic moduli) induced by ASB. As stated above, the framework of large elastic-plastic deformation with anisotropy is put forward.

### 3.1. Large elastic-plastic deformation kinematics including anisotropy

Let $\mathcal{C}_0$ be the initial undeformed configuration of the material, and $\mathcal{C}_t$ its deformed configuration at current time $t$. In order to account for finite elastic–plastic strains — plastic means here inelastic in the sense of both plastic "regular" and damage-induced "singular" terms — the pseudo intermediate configuration $\mathcal{C}_{\text{inter}}$ is introduced by elastic unloading with respect to the current configuration $\mathcal{C}_t$. Because arbitrary local rotations superposed to relaxed state give alternative intermediate configurations, $\mathcal{C}_{\text{inter}}$ is generally non-unique. The deformation gradient $\mathbf{F}$ from $\mathcal{C}_0$ to $\mathcal{C}_t$ is conventionally decomposed as the product $\mathbf{F} = \mathbf{F^e F^{dp}}$ $\left(F_{iJ} = F^e_{i\alpha} F^{dp}_{\alpha J}\right)$, where $\mathbf{F^{dp}}$ denotes the "damage-plastic" transformation from $\mathcal{C}_0$ to $\mathcal{C}_{\text{inter}}$, and $\mathbf{F^e}$ denotes the elastic transformation from $\mathcal{C}_{\text{inter}}$ to $\mathcal{C}_t$.

In the present case, anisotropy is induced by damage (in the form of adiabatic shear bands) during inelastic transformation $\mathbf{F^{dp}}$. It then seems to be natural to define anisotropy in the intermediate configuration $\mathcal{C}_{\text{inter}}$ that becomes henceforth a pseudo-material configuration (see also LUBARDA [17]).

During inelastic deformation $\mathbf{F^{dp}}$, matter is moving with respect to the laboratory fixed frame $\mathcal{S}$. This motion can be decomposed as the sum of the motion of the matter with respect to the anisotropy axes $\mathcal{A}$ and the motion of the anisotropy axes $\mathcal{A}$ with respect to the laboratory frame $\mathcal{S}$. To maintain the axes of anisotropy (damage tensor eigenvectors) $\mathcal{A}$ fixed with respect to the laboratory frame $\mathcal{S}$, it is necessary to rotate at the same time the intermediate configuration $\mathcal{C}_{\text{inter}}$. The rotation needed is then included into elastic transformation $\mathbf{F^e}$. On the other hand, the parameters (vectors and tensors) are expressed with respect to the laboratory frame $\mathcal{S}$. To ensure the double objectivity (invariance under change of frame on the current configuration $\mathcal{C}_t$, and invariance under rotation

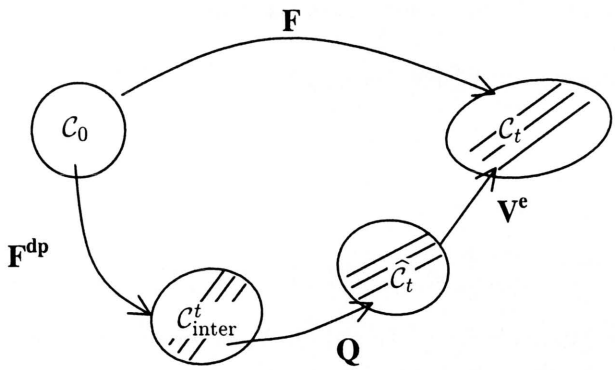


FIG. 4. Intermediate configuration as pseudo-material configuration.

of the intermediate configuration $\mathcal{C}_{\text{inter}}$) of the constitutive model, derivatives in the motion of the matter with respect to the anisotropy axes $\mathcal{A}$ are required [14]. Interference effects of the rotation of anisotropy axes $\mathcal{A}$ with respect to the laboratory frame $\mathcal{S}$ have then to be neutralized.

Let the current configuration $\mathcal{C}_t$ be virtually unstressed by a pure elastic stretching $\mathbf{V^{e-1}}$ to a new configuration called $\widehat{\mathcal{C}}_t$ (Fig. 4). $\mathbf{Q}$ denotes the orthogonal transformation from $\mathcal{C}_{\text{inter}}$ to $\widehat{\mathcal{C}}_t$ ($\mathbf{Q}$ describes the rotation of anisotropy axes $\mathcal{A}$ with respect to the laboratory fixed frame $\mathcal{S}$), and $\mathbf{W} = \dot{\mathbf{Q}}\mathbf{Q}^{\mathbf{T}}$ $\left(W_{ij} = \dot{Q}_{i\alpha}Q^T_{\alpha j}\right)$ denotes the rotation rate relative to these two configurations.
The deformation gradient $\mathbf{F}$ can be written as:

$$F_{iJ} = V^e_{ik}Q_{k\alpha}F^{dp}_{\alpha J} = V^e_{ik}\widetilde{F}^{dp}_{kJ} \tag{3.1}$$

with

$$\overset{\nabla}{\widetilde{F}}{}^{dp}_{iJ} = Q_{i\alpha}F^{dp}_{\alpha J}. \tag{3.2}$$

Introduce the derivative $\overset{\nabla}{\widetilde{\mathbf{F}}}{}^{\mathbf{dp}}$ of $\widetilde{\mathbf{F}}^{\mathbf{dp}}$, objective under any rotation of the intermediate configuration $\mathcal{C}_{\text{inter}}$ as follows:

$$\overset{\nabla}{\widetilde{F}}{}^{dp}_{iJ} = Q_{i\alpha}\dot{F}^{dp}_{\alpha J} = \dot{\widetilde{F}}^{dp}_{iJ} - W_{ik}\widetilde{F}^{dp}_{kJ} \tag{3.3}$$

and denote $\hat{\mathbf{l}}^{\mathbf{dp}}$ the objective damage-plastic velocity gradient:

$$\hat{l}^{dp}_{ij} = Q_{i\alpha}l^{dp}_{\alpha\beta}Q^{dpT}_{\beta j} = \tilde{l}^{dp}_{ij} - W_{ij} \qquad \text{with} \quad \begin{cases} l^{dp}_{\alpha\beta} = \dot{F}^{dp}_{\alpha I}F^{dp-1}_{I\beta}, \\ \tilde{l}^{dp}_{ij} = \dot{\widetilde{F}}^{dp}_{iK}\widetilde{F}^{dp-1}_{Kj}. \end{cases} \tag{3.4}$$

The velocity gradient $\mathbf{l}$ can thus be expressed by:

$$l_{ij} = \dot{F}_{iK}F^{-1}_{Kj} = \dot{V}^e_{ik}V^{e-1}_{kj} + V^e_{im}\dot{\tilde{F}}^{dp}_{mL}\tilde{F}^{dp-1}_{Lp}V^{e-1}_{pj} = \overset{\nabla}{V}{}^e_{ik}V^{e-1}_{kj} + W_{ij} + V^e_{im}\hat{l}^{dp}_{mp}V^{e-1}_{pj} \tag{3.5}$$

where

$$\overset{\nabla}{V}{}^e_{ij} = \dot{V}^e_{ij} - W_{ik}V^e_{kj} + V^e_{ip}W_{pj}. \tag{3.6}$$

As objective derivatives (3.3), (3.4) and (3.6) are constructed with the orthogonal tensor $\mathbf{W}$, they will be called rotational derivatives.

The decomposition of the velocity gradient $\mathbf{l}$ (3.5) into a symmetric part, the strain rate $\mathbf{d}$, and an antisymmetric part, the spin $\boldsymbol{\omega}$, yields:

$$\begin{aligned} d_{ij} &= \left(\overset{\nabla}{V}{}^e_{ik}V^{e-1}_{kj}\right)^S + \left(V^e_{im}\hat{l}^{dp}_{mp}V^{e-1}_{pj}\right)^S, \\ \omega_{ij} &= W_{ij} + \left(\overset{\nabla}{V}{}^e_{ik}V^{e-1}_{kj}\right)^{AS} + \left(V^e_{im}\hat{l}^{dp}_{mp}V^{e-1}_{pj}\right)^{AS}. \end{aligned} \tag{3.7}$$

The elastic strain rate $\mathbf{d^e}$ and spin $\boldsymbol{\omega}^{\mathbf{e}}$, and the inelastic strain rate $\mathbf{d^{dp}}$ and spin $\boldsymbol{\omega}^{\mathbf{dp}}$ are extracted from (3.7) as follows:

$$\begin{aligned} d^e_{ij} &= \left(\overset{\nabla}{V}{}^e_{ik}V^{e-1}_{kj}\right)^S \\ \omega^e_{ij} &= \left(\overset{\nabla}{V}{}^e_{ik}V^{e-1}_{kj}\right)^{AS} \end{aligned} \tag{3.8}$$

and

$$\begin{aligned} d^{dp}_{ij} &= \left[V^e_{im}\tilde{d}^{dp}_{mp}V^{e-1}_{pj}\right]^S + \left[V^e_{in}\hat{\omega}^{dp}_{nq}V^{e-1}_{qj}\right]^S \\ \omega^{dp}_{ij} &= \left[V^e_{im}\tilde{d}^{dp}_{mp}V^{e-1}_{pj}\right]^{AS} + \left[V^e_{in}\hat{\omega}^{dp}_{nq}V^{e-1}_{qj}\right]^{AS} \end{aligned}$$

where

$$\begin{aligned} \tilde{d}^{dp}_{ij} &= \left(\tilde{l}^{dp}_{ij}\right)^S = \left(\hat{l}^{dp}_{ij}\right)^S, \\ \hat{\omega}^{dp}_{ij} &= \left(\hat{l}^{dp}_{ij}\right)^{AS}. \end{aligned} \tag{3.9}$$

According to (3.7) and (3.8), the total strain rate $\mathbf{d}$ and spin $\boldsymbol{\omega}$ are given by:

$$\begin{aligned} d_{ij} &= d^e_{ij} + d^{dp}_{ij}, \\ \omega_{ij} &= W_{ij} + \omega^e_{ij} + \omega^{dp}_{ij}. \end{aligned} \tag{3.10}$$

The rotation rate $\mathbf{W}$ of the damage tensor eigenvectors (anisotropy axes) is obtained from $(3.10)_2$ by:

$$W_{ij} = \omega_{ij} - \left(\omega^e_{ij} + \omega^{dp}_{ij}\right). \tag{3.11}$$

As previously written by MANDEL [14], constitutive relations for anisotropic media need not only the definition of the strain rate but also that of the spin. The laws concerning $\boldsymbol{\omega}^{\mathbf{e}}$ and $\boldsymbol{\omega}^{\mathbf{dp}}$ are indeed required to achieve the calculation of the rotational derivatives (see also DAFALIAS [18]).

### 3.2. Constitutive model

The state of the material is described at the intermediate configuration $\mathcal{C}_{\text{inter}}$ employing the following variables:

- elastic right Cauchy-Green tensor $C^e_{\alpha\beta} = F^{eT}_{\alpha i} F^e_{i\beta} = U^e_{\alpha\gamma} U^e_{\gamma\beta}$
- absolute "regular" temperature $T$
- scalar isotropic strain-hardening variable $p$
- internal damage variable $D_{\alpha\beta} = d.n_\alpha n_\beta$ with $d = d(T^*, ...)$.

When the corresponding state variables are expressed in the current configuration $\mathcal{C}_t$, they must be invariant under rotation of the intermediate configuration $\mathcal{C}_{\text{inter}}$. The elastic left Cauchy-Green tensor $\mathbf{b}^{\mathbf{e}}$ satisfies this condition.

Anisotropy evolves during the inelastic transformation $\mathbf{F}^{\mathbf{dp}}$. Through a rotation $\mathbf{Q}$ of the intermediate configuration $\mathcal{C}_{\text{inter}}$, the vector $\mathbf{n}$ is transformed into $\widetilde{\mathbf{n}}$ as $\widetilde{\mathbf{n}} = \mathbf{Q}\mathbf{n}$ ($\widetilde{n}_i = Q_{i\alpha} n_\alpha$). Then

$$D_{\alpha\beta} = d \cdot n_\alpha n_\beta = d Q^T_{\alpha i} \widetilde{n}_i Q^T_{\beta j} \widetilde{n}_j = d Q^T_{\alpha i} \widetilde{n}_i \widetilde{n}_j Q_{j\beta} = Q^T_{\alpha i} \widetilde{D}_{ij} Q_{j\beta}.$$

Consider the new damage variable $\widetilde{\mathbf{D}}$ invariant under rotation of the intermediate configuration $\mathcal{C}_{\text{inter}}$ as:

$$\widetilde{D}_{ij} = d\widetilde{n}_i \widetilde{n}_j = Q_{i\alpha} D_{\alpha\beta} Q^T_{\beta j}. \tag{3.12}$$

The state of the material may be described at the current configuration $\mathcal{C}_t$ employing the following variables:

- elastic left Cauchy-Green tensor $b^e_{ij} = F^e_{i\alpha} F^{eT}_{\alpha j} = V^e_{ik} V^e_{kj}$
- absolute "regular" temperature $T$
- scalar isotropic strain hardening variable $p$
- internal damage variable $\widetilde{D}_{ij} = d\widetilde{n}_i \widetilde{n}_j = Q_{i\alpha} D_{\alpha\beta} Q^T_{\beta j}$

The objective rotational derivative of $\widetilde{\mathbf{D}}$ (3.12) is obtained by neutralizing the rotation $\mathbf{Q}$:

$$\overset{\nabla}{\widetilde{D}}_{ij} = Q_{i\alpha} \dot{D}_{\alpha\beta} Q^T_{\beta j} = \dot{\widetilde{D}}_{ij} - W_{ik} \widetilde{D}_{kj} + \widetilde{D}_{ip} W_{pj}. \tag{3.13}$$

The thermo-elastic response of the anisotropic medium is supposed to be described by a thermodynamic potential, namely the free energy per unit unstressed volume $\rho^p\psi(\mathbf{C^e}, T; p, \mathbf{D})$, where $\rho^p$ represents the density in the intermediate configuration and $\psi(\mathbf{C^e}, T; p, \mathbf{D})$ the specific free energy. Assuming incompressible inelastic deformation $\left(\det \mathbf{F^{dp}} = 1\right)$, initial and unstressed volume are equal, then $\rho_0\psi(\mathbf{C^e}, T; p, \mathbf{D}) = \rho^p\psi(\mathbf{C^e}, T; p, \mathbf{D})$, where $\rho_0$ represents the initial density. Material frame-indifference requirement is ensured through the invariance of the thermodynamic potential by any rotation of the intermediate configuration:

$$\rho_0\psi\left(\mathbf{C^e}, T; p, \mathbf{D}\right) = \rho_0\psi\left(\mathbf{QC^eQ^T}, T; p, \mathbf{QDQ^T}\right) = \rho_0\psi\left(\mathbf{b^e}, T; p, \widetilde{\mathbf{D}}\right).$$

The free energy per unit initial volume is further decomposed into a reversible part $\rho_0\psi^e(\mathbf{b^e}, T; \widetilde{\mathbf{D}})$, namely the elastic potential, and a stored energy part $\rho_0\psi^p(T; p, \widetilde{\mathbf{D}})$ as follows:

$$\rho_0\psi\left(\mathbf{b^e}, T; p, \widetilde{\mathbf{D}}\right) = \rho_0\psi^e\left(\mathbf{b^e}, T; \widetilde{\mathbf{D}}\right) + \rho_0\psi^p\left(T; p, \widetilde{\mathbf{D}}\right). \tag{3.14}$$

The elastic potential includes the initial isotropic linear thermo-elasticity of the sound material and damage-induced anisotropic elastic effects in the degraded material. It is constructed from the theory of isotropic scalar functions of several tensorial arguments (see BOEHLER [19]). The elastic degradation is described as dependent on $\widetilde{\mathbf{D}}$, thus comprising damage-induced orthotropy effects via two terms involving material constants $a$ and $b$ below, see also DRAGON *et al.* [13]. It is assumed that possible interactions between different band clusters are not taken into account. The form (3.15) below is thus limited to the first order in $\widetilde{\mathbf{D}}$.

The elastic potential is assumed in the form:

$$\rho_0\psi^e = \frac{\lambda}{2}e^e_{ii}e^e_{jj} + \mu e^e_{ij}e^e_{ji} - \alpha K e^e_{ii}\Delta T - \frac{\rho_0 C}{2T_0}\Delta T^2 - a e^e_{kk}e^e_{ij}\widetilde{D}_{ji} - 2b e^e_{ij}e^e_{jk}\widetilde{D}_{ki} \tag{3.15}$$

with

$$e^e_{ij} = g\left(b^e_{ij}\right), \qquad \Delta T = T - T_0, \qquad K = \frac{3\lambda + 2\mu}{3},$$

where $\mathbf{e^e}$ represents a spatial elastic strain measure, a function of $\mathbf{b^e}$ (see Eq. (3.23) below), which satisfies the hypotheses mentioned above concerning the elastic potential under the assumption of small elastic strains. The expression of corresponding stress tensor is given in Eq. $(3.26)_1$ below. In this context, $\lambda$ and $\mu$ represent Lamé's coefficients, $K$ the bulk modulus, $\alpha$ the thermal dilatation coefficient, $\rho_0$ the initial density, $C$ the heat capacity, $a$ and $b$ the constants

mentioned above related to elastic energy degradation caused by adiabatic shear banding.

The stored energy reflects the competition that takes place inside the material between hardening and softening. Hardening is a consequence of the micromechanisms of "regular" plasticity, while softening is due to heating on the one hand and to current ASB-related damage on the other one. During their evolution (formation and propagation), ASB modify internal stresses. In this sense, one can assume that damage acts much like temperature to release the stored energy. These considerations justify the choice of a multiplicative decomposition of the hardening into respective heating and damage contributions. Note that in the expression (3.16) below, the introduction in the stored energy of the 2nd invariant of the damage variable $\widetilde{\mathbf{D}}$ allows to produce some effects of band interaction.

The stored energy is written as follows:

$$\rho_0\psi^p = R_\infty\left[p+\frac{1}{k}\exp(-kp)\right]\exp(-\gamma T)\exp\left(-d_1\widetilde{D}_{ii}-\frac{d_2}{2}\widetilde{D}_{ij}\widetilde{D}_{ji}\right) \tag{3.16}$$

where $R_\infty$ represents the saturation stress, $k$ the plastic hardening parameter linked to the initial hardening modulus, $\gamma$ the thermal softening parameter, $d_1$ and $d_2$ the damage (ASB)-related softening constants.

A model consistent with irreversible thermodynamic framework should satisfy the Clausius-Duhem dissipation inequality. The latter is written below in the current configuration:

$$\mathcal{D}_{\text{int}} = \sigma_{ij}d_{ji} - \rho\left(\dot{\psi}+s\dot{T}\right) \geq 0 \tag{3.17}$$

where $\boldsymbol{\sigma}$ represents the thermo-elastic (reversible) Cauchy stress tensor, $\rho$ the current density, and $s$ the entropy.

Chain rule applied for differentiation of the free energy gives:

$$\dot{\psi} = \frac{\partial\psi}{\partial b^e_{ij}}\dot{b}^e_{ji} + \frac{\partial\psi}{\partial T}\dot{T} + \frac{\partial\psi}{\partial p}\dot{p} + \frac{\partial\psi}{\partial\widetilde{D}_{ij}}\dot{\widetilde{D}}_{ji}\,. \tag{3.18}$$

Nevertheless, the invariance of $\dot{\psi}$ requires objective derivatives for the tensors. To avoid surplus contribution to dissipated energy, rotational derivatives are used following DOGUI and SIDOROFF [20]:

$$\dot{\psi} = \frac{\partial\psi}{\partial b^e_{ij}}\overset{\nabla}{b}{}^e_{ji} + \frac{\partial\psi}{\partial T}\dot{T} + \frac{\partial\psi}{\partial p}\dot{p} + \frac{\partial\psi}{\partial\widetilde{D}_{ij}}\overset{\nabla}{\widetilde{D}}_{ji}\,. \tag{3.19}$$

In the foregoing, the derivative $\overset{\nabla}{\mathbf{b}^e}$ is related to the strain rate $\mathbf{d}$ by:

$$\overset{\nabla}{b}{}^e_{ij} = \left(V^e_{ik}\overset{\nabla}{V}{}^e_{kj}\right) = 2V^e_{ik}d_{kl}V^e_{lj} - \left(b^e_{im}\hat{l}^{dp}_{mj} + \hat{l}^{dp}_{in}b^e_{nj}\right). \tag{3.20}$$

Gibbs relation and Clausius-Duhem inequality are finally written as:

$$\begin{aligned} \rho\dot{\psi} &= -\rho s\dot{T} + \sigma_{ij}\left(d_{ji} - \tilde{d}^{dp}_{ji}\right) + R\dot{p} - \widetilde{K}_{ij}\overset{\nabla}{\widetilde{D}}_{ji}\,, \\ \mathcal{D}_{\text{int}} &= \sigma_{ij}\tilde{d}^{dp}_{ji} - R\dot{p} + \widetilde{K}_{ij}\overset{\nabla}{\widetilde{D}}_{ji} \geq 0, \end{aligned} \tag{3.21}$$

where $\boldsymbol{\sigma}$ represents the thermo-elastic Cauchy stress tensor, $R$ the isotropic hardening conjugate force, $\widetilde{\mathbf{K}}$ the damage conjugate force, and $s$ the entropy.

The conjugate forces are derived from the thermodynamic potential:

$$\begin{aligned} \tau_{ij} &= J\sigma_{ij} = 2\rho_0 V^e_{ik}\frac{\partial\psi}{\partial b^e_{km}}V^e_{mj} = 2\rho_0 b^e_{ip}\frac{\partial\psi}{\partial b^e_{pj}}\,, \\ r &= JR = \rho_0\frac{\partial\psi}{\partial p}\,, \\ \widetilde{k}_{ij} &= J\widetilde{K}_{ij} = -\rho_0\frac{\partial\psi}{\partial\widetilde{D}_{ij}}\,, \\ \rho_0 s &= -\rho_0\frac{\partial\psi}{\partial T}\,, \end{aligned} \tag{3.22}$$

where $\tau$ represents the thermo-elastic Kirchhoff stress tensor, and $J$ the Jacobian determinant of $\mathbf{F}$.

As stated above, the class of materials considered here implies small elastic strains. The elastic strain measure $\mathbf{e^e}$ is chosen herein as follows:

$$e^e_{ij} = \frac{1}{2}\ln b^e_{ij} = \ln V^e_{ij}\,. \tag{3.23}$$

Derivation of $\mathbf{e^e}$ yields an equality between the rotational derivative $\overset{\nabla}{\mathbf{e}}^{\mathbf{e}}$ and the elastic strain rate $\mathbf{d^e}$:

$$\overset{\nabla}{e}{}^e_{ij} = d^e_{ij} = \dot{e}^e_{ij} - W_{ik}e^e_{kj} + e^e_{ip}W_{pj}\,. \tag{3.24}$$

On the other hand, the thermo-elastic Kirchhoff stress tensor is simply expressed as follows:

$$\tau_{ij} = \rho_0\frac{\partial\psi}{\partial e^e_{ij}}\,. \tag{3.25}$$

The conjugate forces (3.22) are henceforth expressed by:

$$
\begin{aligned}
\tau_{ij} &= \lambda e^e_{kk}\delta_{ij} + 2\mu e^e_{ij} - \alpha K \Delta T \delta_{ij} \\
&\quad - a\left(e^e_{mn}\widetilde{D}_{nm}\delta_{ij} + e^e_{kk}\widetilde{D}_{ij}\right) - 2b\left(e^e_{ik}\widetilde{D}_{kj} + \widetilde{D}_{ik}e^e_{kj}\right), \\
r &= R_\infty\left[1 - \exp\left(-kp\right)\right]\exp(-\gamma T)\exp\left(-d_1\widetilde{D}_{kk} - \frac{d_2}{2}\widetilde{D}_{kl}\widetilde{D}_{lk}\right), \\
\tilde{k}_{ij} &= a e^e_{kk}e^e_{ij} + 2b e^e_{ik}e^e_{kj} + R_\infty\left[p + \frac{1}{k}\exp(-kp)\right] \\
&\quad \cdot \exp(-\gamma T)\exp\left(-d_1\widetilde{D}_{kk} - \frac{d_2}{2}\widetilde{D}_{kl}\widetilde{D}_{lk}\right)\left[d_1\delta_{ij} + d_2\widetilde{D}_{ij}\right], \\
\rho_0 s &= \alpha K e^e_{kk} + \frac{\rho C}{T_0}\Delta T \\
&\quad + \gamma R_\infty\left[p + \frac{1}{k}\exp(-kp)\right]\exp(-\gamma T)\exp\left(-d_1\widetilde{D}_{kk} - \frac{d_2}{2}\widetilde{D}_{kl}\widetilde{D}_{lk}\right).
\end{aligned}
\tag{3.26}
$$

Isotropic heating and anisotropic damage contribute to reduction of the stress level $\tau_{ij}\left(\mathbf{e}^{\mathbf{e}}, T; \widetilde{\mathbf{D}}\right)$ $(3.26)_1$. Positive constants $a$ and $b$ contribute both to reduction of the Young's modulus, while $b$ is alone related to the decrease of the shear modulus (see also Sec. 5).

Without heating and damage (isothermal conditions in quasi-static configuration), the conjugate force $r(T; p, \widetilde{\mathbf{D}})$ in $(3.26)_2$, relative to isotropic hardening, tends to the saturation stress $R_\infty \exp(-\gamma T_0)$. This force increases during pure hardening but decreases with heating and damage, describing the competition between hardening and softening.

The damage conjugate force $\widetilde{\mathbf{k}}(\mathbf{e}^{\mathbf{e}}, T; p, \widetilde{\mathbf{D}})$ — the energy release rate with respect to $\widetilde{\mathbf{D}}$ — $(3.26)_3$ includes the first contribution from the reversible part of the free energy, and the second one from the stored energy. The corresponding terms represent respectively elastic and stored energy release rates. It is noteworthy that both contributions to the damage conjugate force exist before damage inception. It is assumed that a finite supply of energy is necessary to activate the damage process.

The objective formulation of the incremental constitutive model can be written in a compact form as follows:

$$
\begin{Bmatrix} +\overset{\nabla}{\tau}_{ij} \\ +\dot{r} \\ -\overset{\nabla}{\tilde{k}}_{ij} \\ -\rho_0\dot{s} \end{Bmatrix} = \begin{bmatrix} C_{ijkl} & 0 & E_{ijkl} & J_{ij} \\ 0 & Q & A_{kl} & S \\ E_{ijkl} & A_{ij} & L_{ijkl} & V_{ij} \\ J_{kl} & S & V_{kl} & X \end{bmatrix} \begin{Bmatrix} d_{kl} - \tilde{d}^{dp}_{kl} \\ \dot{p} \\ \overset{\nabla}{\widetilde{D}}_{kl} \\ \dot{T} \end{Bmatrix}. \tag{3.27}
$$

with

$$C_{ijkl} = \rho_0 \frac{\partial^2 \psi}{\partial e^e_{ij} \partial e^e_{kl}}; \qquad E_{ijkl} = \rho_0 \frac{\partial^2 \psi}{\partial e^e_{ij} \partial \widetilde{D}_{kl}}; \qquad J_{ij} = \rho_0 \frac{\partial^2 \psi}{\partial e^e_{ij} \partial T}; \qquad Q = \rho_0 \frac{\partial^2 \psi}{\partial p^2}$$

and

$$S = \rho_0 \frac{\partial^2 \psi}{\partial p \partial T}; \qquad A_{ij} = \rho_0 \frac{\partial^2 \psi}{\partial p \partial \widetilde{D}_{ij}}; \qquad L_{ijkl} = \rho_0 \frac{\partial^2 \psi}{\partial \widetilde{D}_{ij} \partial \widetilde{D}_{kl}};$$

$$V_{ij} = \rho_0 \frac{\partial^2 \psi}{\partial \widetilde{D}_{ij} \partial T}; \qquad X = \rho_0 \frac{\partial^2 \psi}{\partial T^2}$$

(see Appendix A for further details).

Since we have assumed small elastic strains ($V^e_{ij} \approx \delta_{ij} + \varepsilon_{ij}$ with $\varepsilon_{ij}\varepsilon_{ji} \ll 1$), expressions (3.8) are reduced to:

$$\left\{ \begin{array}{lcl} d^e_{ij} & = & \overset{\nabla}{V}{}^e_{ij} \\ \omega^e_{ij} & = & 0 \end{array} \right. \qquad \left\{ \begin{array}{lcl} d^{dp}_{ij} & = & \widetilde{d}^{dp}_{ij}, \\ \omega^{dp}_{ij} & = & \widehat{\omega}^{dp}_{ij}. \end{array} \right. \tag{3.28}$$

As a consequence, the rotation rate (3.11), needed for the rotational derivatives, becomes:

$$W_{ij} = \omega_{ij} - \omega^{dp}_{ij}. \tag{3.29}$$

As stated before, the constitutive model requires a law specifying $\boldsymbol{\omega^{dp}}$ in addition to the conventional complementary laws.

Another consequence of the small elastic strains assumption concerns the form (3.27) which becomes:

$$\left\{ \begin{array}{c} +\overset{\nabla}{\tau}_{ij} \\ +\dot{r} \\ -\overset{\nabla}{\tilde{k}}_{ij} \\ -\rho_0 \dot{s} \end{array} \right\} = \left[ \begin{array}{cccc} C_{ijkl} & 0 & E_{ijkl} & J_{ij} \\ 0 & Q & A_{kl} & S \\ E_{ijkl} & A_{ij} & L_{ijkl} & V_{ij} \\ J_{kl} & S & V_{kl} & X \end{array} \right] \left\{ \begin{array}{c} d^e_{kl} \\ \dot{p} \\ \overset{\nabla}{\widetilde{D}}_{kl} \\ \dot{T} \end{array} \right\}. \tag{3.30}$$

The dissipation can be decomposed into a "regular" part directly linked to plasticity and a "singular" part resulting from band formation:

$$\mathcal{D}_{\text{int}} = \mathcal{D}_{\text{reg}} + \mathrm{D}_{\text{sing}}. \tag{3.31}$$

The respective contributions are as follows:

$$\begin{aligned} \mathcal{D}_{\text{reg}} &= \sigma_{ij} d^p_{ji} - R\dot{p}, \\ \mathcal{D}_{\text{sing}} &= \sigma_{ij} d^d_{ji} + F_{ij} \overset{\nabla}{\widetilde{D}}_{ji}, \end{aligned} \tag{3.32}$$

where $\mathbf{d^p}$ represents the "regular" plastic strain rate, and $\mathbf{d^d}$ the "singular" damage-induced strain rate.

The effects of "singular" heating localized inside the band cluster are included, by definition of the damage variable (2.1)–(2.2), in the scalar damage density $d^{\alpha}$ (2.2), evolving with the ongoing deterioration. "Regular" heating caused by plasticity outside the bands is then expressed by the common relation established with the adiabaticity assumption:

$$\rho_0 C\dot{T} = \sigma_{ij} d^p_{ji} - R\dot{p}. \tag{3.33}$$

One may distinguish three stages during the deformation progress: before the onset of localization, "regular" plasticity is the only dissipative mechanism; just after the onset of localization, both mechanisms, namely "regular" plasticity and "singular" damage coexist; when localization advances, ASB damage process becomes progressively the prevalent dissipative mechanism. Using a single yield function that includes both the plasticity and damage effects, seems to be suitable to favour such a chronology in the evolution of "regular" and "singular" variables.

The following extended form of the plasticity and damage loading function $\mathcal{F}$ is postulated:

$$\mathcal{F}\left(\tau_{ij}, r, \tilde{k}_{ij}\right) = \hat{J}_2^s\left(\tau_{ij}, \tilde{k}_{ij}\right) - (R_0 + r), \tag{3.34}$$

where the generalized 2nd invariant $\hat{J}_2^s\left(\tau, \widetilde{\mathbf{k}}\right)$ incorporates the damage conjugate force $\widetilde{\mathbf{k}}\left(\widetilde{\mathbf{D}}, ...\right)$ as follows:

$$\hat{J}_2^s\left(\tau_{ij}, \tilde{k}_{ij}\right) = \sqrt{\frac{3}{2} s_{ij} P_{ijkl}\left(\tilde{k}_{mn}\right) s_{kl}}. \tag{3.35}$$

In (3.35) $\mathbf{s}$ represents the deviatoric part of the Kirchhoff stress tensor, and $\mathbf{P}\left(\widetilde{\mathbf{k}}\right)$ the 4th order tensor inducing anisotropy of plastic flow.

The tensor $\mathbf{P}\left(\widetilde{\mathbf{k}}\right)$, see (3.37) below, includes the first term relative to conventional plasticity without damage and the second one relative to damage-induced effects on the plastic flow. The evolution laws (3.43), which are derived from the normality rule, require by definition the collinearity of the "regular" plastic strain rate $\mathbf{d^p}$ to the deviatoric part $\mathbf{s}$ of the Kirchhoff stress tensor, the collinearity of the "singular" damage-induced strain rate $\mathbf{d^d}$ to the orientation tensor $\mathbf{M}$ (according to $(2.3)_1$), and finally the collinearity of the damage rate $\overset{\nabla}{\widetilde{\mathbf{D}}}$ to the orientation tensor $\mathbf{N}$ for conservative damage growth configuration

considered here (according to $(2.1)_1$). Conjugate forces $\left(\mathbf{s}, \widetilde{\mathbf{k}}\right)$ and "orientation" tensors $(\mathbf{s}, \mathbf{M}, \mathbf{N})$ are then associated in the generalized $2^{\text{nd}}$ invariant (3.35) to satisfy such conditions. The continuity of stress at the onset of damage is preserved. In the expression of $\mathbf{P}$, the damage driving force $\widetilde{\mathbf{k}}$ intervenes via the expression $\text{Tr}\left(\widetilde{\mathbf{k}}^{+}\mathbf{N}\right)$, where $\text{Tr}\left(\widetilde{\mathbf{k}}^{+}\mathbf{N}\right)$ represents the difference between the current value $\text{Tr}\left(\widetilde{\mathbf{k}}\mathbf{N}\right)$ and the corresponding one at the incipience of damage $k_{\text{inc}} = \text{Tr}\left(\widetilde{\mathbf{k}}\mathbf{N}\right)_{inc}$:

$$\tilde{k}_{ij}^{+} N_{ji} = \left\langle \tilde{k}_{ij} N_{ji} - k_{\text{inc}} \right\rangle, \tag{3.36}$$

where the bracket $\langle \cdot \rangle$ defines the ramp function. To determine $k_{\text{inc}}$, an auxiliary analysis based on perturbation method will be conducted in Section 4 for a particular loading path.

On the other hand, to ensure the concomitance of both damage-induced rates $\mathbf{d}^{\mathbf{d}}$ and $\overset{\nabla}{\widetilde{\mathbf{D}}}$, the polynomial in $\text{Tr}\left(\widetilde{\mathbf{k}}^{+}\mathbf{N}\right)$ specified below in (3.37) starts with the exponent $q = 2$ (see $(3.43)_2$ and $(3.43)_4$ below).

The $4^{\text{th}}$ order tensor $\mathbf{P}\left(\widetilde{\mathbf{k}}\right)$ is finally represented as follows:

$$P_{ijkl} = \frac{1}{2}(\delta_{ik}\delta_{jl} + \delta_{il}\delta_{jk}) + 2\sum_{q=2}^{N} \eta_q \left(\tilde{k}_{mn}^{+} N_{nm}\right)^q M_{ij} M_{kl}\,. \tag{3.37}$$

The function $R_0$ in (3.34), which represents the radius of the Huber-Von Mises cylinder without hardening in the stress space, must account for heating and damage softening. A form close to the hardening conjugate force $(3.26)_2$ is adopted:

$$R_0 = R_i \exp(-\gamma T) \exp\left(-d_1 \widetilde{D}_{kk} - \frac{d_2}{2} \widetilde{D}_{mn} \widetilde{D}_{nm}\right), \tag{3.38}$$

where $R_i$ represents the internal stress, $\gamma$ the thermal softening parameter, $d_1$ and $d_2$ the damage (ASB) softening parameters. The inelasticity criterion $\mathcal{F} = 0$ is assumed. The viscoplastic flow and (viscous) damage growth domain is thus $\mathcal{F} \geq 0$.

The existence of a viscoplastic potential of PERZYNA's type [21] is assumed:

$$\phi_p^c = \frac{Y}{n+1} \left\langle \frac{\mathcal{F}}{Y} \right\rangle^{n+1} \tag{3.39}$$

where $\mathcal{F}$ represents the yield function, $Y$ and $n$ viscous parameters relative to "regular" plasticity, and the bracket $\langle \cdot \rangle$ the ramp function. Time-dependent

shear banding (damage mechanism considered here) is an evident consequence of thermo-viscoplastic flow. The viscous damage potential is thus chosen close to the plastic one (3.39):

$$\phi_d^c = \frac{Z}{m+1}\left\langle \frac{\mathcal{F}}{Z} \right\rangle^{m+1} \tag{3.40}$$

where $\mathcal{F}$ represents the yield function, $Z$ and $m$ viscous parameters relative to "singular" damage, and the bracket $\langle\cdot\rangle$ is the ramp function.

Evolution laws are consequently derived from the normality rule:

$$\begin{aligned} d_{ij}^{dp} &= d_{ij}^{p} + d_{ij}^{d} = \frac{\partial \phi_p^c}{\partial \tau_{ij}} = \Lambda^p \frac{\partial \mathcal{F}}{\partial \tau_{ij}}\,; \\ -\dot{p} &= \frac{\partial \phi_p^c}{\partial r} = \Lambda^p \frac{\partial \mathcal{F}}{\partial r}\,; \qquad \overset{\nabla}{\tilde{D}}_{ij} = \frac{\partial \phi_d^c}{\partial \tilde{k}_{ij}} = \Lambda^d \frac{\partial \mathcal{F}}{\partial \tilde{k}_{ij}} \end{aligned} \tag{3.41}$$

with the viscoplasticity and viscous damage respective multipliers expressed by:

$$\Lambda^p = \left\langle \frac{\partial \phi_p^c}{\partial \mathcal{F}} \right\rangle = \left\langle \frac{\mathcal{F}}{Y} \right\rangle^n ; \qquad \Lambda^d = \left\langle \frac{\partial \phi_d^c}{\partial \mathcal{F}} \right\rangle = \left\langle \frac{\mathcal{F}}{Z} \right\rangle^m . \tag{3.42}$$

The corresponding fluxes are finally written as follows:

$$\begin{aligned} d_{ij}^{p} &= \frac{3}{2}\Lambda^p \frac{s_{ij}}{\widehat{J}_2^s}\,, \\ d_{ij}^{d} &= 3\Lambda^p \frac{\sum_{q=2}^{N} \eta_q \left(\tilde{k}_{mn}^{+} N_{nm}\right)^q s_{kl} M_{kl}}{\widehat{J}_2^s} M_{ij}\,, \\ \dot{p} &= \Lambda^p, \\ \overset{\nabla}{\tilde{D}}_{ij} &= \frac{3}{2}\Lambda^d \frac{\sum_{q=2}^{N} q \cdot \eta_q \left(\tilde{k}_{mn}^{+} N_{nm}\right)^{q-1} (s_{kl} M_{kl})^2}{\widehat{J}_2^s} N_{ij}\,. \end{aligned} \tag{3.43}$$

As discussed above, the rates $\mathbf{d^p}$, $\mathbf{d^d}$ and $\overset{\nabla}{\tilde{\mathbf{D}}}$ are respectively collinear to $\mathbf{s}$, $\mathbf{M}$ and $\mathbf{N}$. The adiabatic shear banding process which generates the damage-induced strain rate $\mathbf{d^d}$ modifies the initial direction of the inelastic strain rate $\mathbf{d^{dp}}$. The norms of the damage-induced rates $\mathbf{d^d}$ and $\overset{\nabla}{\tilde{\mathbf{D}}}$ contain both a part relative to the damage conjugate force $\tilde{\mathbf{k}}$ (via the expression $\mathrm{Tr}\left(\tilde{\mathbf{k}}^{+}\mathbf{N}\right)$) and another part relative to the resolved shear stress $\tau_{\mathrm{res}} = \mathrm{Tr}\,(\mathbf{sM})$ (in the band cluster plane).

The damage conjugate force $\tilde{\mathbf{k}}$ is actually the preponderant driving force of the damage-induced strain rate $\mathbf{d^d}$ (see the expression $(3.43)_2$ above), while the damage conjugate force $\tilde{\mathbf{k}}$ and the resolved shear stress $\tau_{\text{res}}$ keep approximately the same weight in the expression $(3.43)_4$ governing the magnitude of the damage rate $\overset{\nabla}{\tilde{\mathbf{D}}}$, recalling that damage is primarily the consequence of a shearing process.

Let the inelastic velocity gradient $\mathbf{l^{dp}}$ be decomposed into a "regular" contribution $\mathbf{l^p}$ and a "singular" one $\mathbf{l^d}$:

$$l_{ij}^{dp} = l_{ij}^{p} + l_{ij}^{d}\,. \tag{3.44}$$

In the absence of damage ($\mathbf{l^d} = \mathbf{0}$), the "regular" structure of matter can be supposed to be approximately statistically isotropic, what implies that $\omega^{\mathbf{p}} = \mathbf{0}$, see MANDEL [22]. The rate $\mathbf{W}$ is in this case equal to the spin $\omega$: rotational derivatives are then simply the Zaremba-Jaumann derivatives. In the presence of damage, the damage-induced velocity gradient $\mathbf{l^d}$ generates the spin $\omega^{\mathbf{d}}$. Assuming that the effects of the distorsion caused by the presence of ASB are concentrated in their close vicinity, "regular" matter is supposed to be globally weakly affected. In this sense, the "regular" plastic spin $\omega^{\mathbf{p}}$ can be neglected with respect to the "singular" damage-induced spin $\omega^{\mathbf{d}}$. The rotation rate (3.29) is thus reduced to:

$$W_{ij} = \omega_{ij} - \omega_{ij}^{d}. \tag{3.45}$$

The analogy drawn in Section 2 between a band cluster and a "super-dislocation" is used here again to postulate the "singular" contribution $\mathbf{l^d}$ as:

$$l_{ij}^{d} \propto \sum_{\alpha} \dot{\gamma}^{\alpha} g_i^{\alpha} n_j^{\alpha}. \tag{3.46}$$

The partition of the damage-induced velocity gradient $\mathbf{l^d}$ (3.46) gives the damage-induced strain rate $\mathbf{d^d}$ and the damage-induced spin $\omega^{\mathbf{d}}$ as follows:

$$\begin{aligned} d_{ij}^{d} &\propto \sum_{\alpha} \dot{\gamma}^{\alpha} \left(g_i^{\alpha} n_j^{\alpha}\right)^{S}, \\ \omega_{ij}^{d} &\propto \sum_{\alpha} \dot{\gamma}^{\alpha} \left(g_i^{\alpha} n_j^{\alpha}\right)^{AS}. \end{aligned} \tag{3.47}$$

According to relation $(3.43)_2$, which expresses the damage-induced strain rate $\mathbf{d^d}$, one can express the damage-induced spin $\omega^{\mathbf{d}}$ $(3.47)_2$ as:

$$\omega_{ij}^{d} = 3\Lambda^{p} \frac{\sum_{r=2}^{N} \eta_r \left(\tilde{k}_{pq}^{+} N_{qp}\right)^{r} s_{kl} M_{kl}}{\hat{J}_2^{s}} T_{ij} \tag{3.48}$$

where

$$T_{ij} = (g_i n_j)^{AS} = \frac{1}{2}(g_i n_j - g_j n_i).$$

As stressed before, material behaviour, described via the incremental law (3.30), requires objective rotational derivatives. From the analogy of damage-induced viscoplastic deformation with finite plastic distorsion in crystals, the above evaluation of the damage-induced spin has been obtained, thus completing the constitutive relations.

## 4. Damage incipience via simplified perturbation analysis

The constitutive model is now completed by a damage incipience criterion based on a simplified analysis of material instability using the linear perturbation method.

The method is in general applied in the case of simple shear under constant velocity boundary conditions. Assuming negligible elastic effects, laminar viscoplastic flow and adiabatic conditions, the problem can be reduced to a one-dimensional formulation, see e.g. BAI [3], CLIFTON *et al.* [23], MOLINARI [24], and SHAWKI and CLIFTON [25]. Admitting analytical solutions, the linear perturbation method provides in this case a criterion of instability onset, which is interpreted as the incipience of the adiabatic shear banding process. Nevertheless, instability does not rigorously imply localization [24]. This means that the use of the method gives a "lower" bound of the deformation localization incipience.

An auxiliary simplified analysis performed here is intended to help to establish damage incipience threshold and its form based on more pertinent indications than the purely phenomenological formulation. The output of the analysis presented below will be limited to a particular loading path. Instead of rigorous instability search ("lower" bound for localization mentioned above), the aim is to search a more realistic ("upper" bound) evaluation for localization incipience. The hypotheses taken further favour delaying the strong localization onset with respect to the supposed instability onset.

As mentioned in Sec. 3, this auxiliary analysis allows actually to determine $k_{\text{inc}} = \text{Tr}\left(\widetilde{\mathbf{k}}\mathbf{N}\right)_{\text{inc}}$ in (3.36), which activates the damage-related rates $\mathbf{d}^{\mathbf{d}}$ and $\overset{\nabla}{\widetilde{\mathbf{D}}}$ (see expressions $(3.43)_2$ and $(3.43)_4$), from mechanical considerations. In the absence of damage, assuming negligible elastic effects, the governing equations may be written as:

$$\tau_{ij,j} - \rho_0 \dot{v}_i = 0,$$

$$\rho_0 C\dot{T} - \kappa T_{,kk} - (J_2 - r)\dot{p} = 0, \tag{4.1}$$

$$
\begin{aligned}
\frac{1}{2}(v_{i,j}+v_{j,i})-\frac{3}{2}\dot{p}\frac{s_{ij}}{J_2} &= 0,\\
\dot{p}-\Lambda^p(\tau_{ij},p,T) &= 0,
\end{aligned}
\tag{4.1 [cont.]}
$$

where $J_2=\sqrt{\frac{3}{2}s_{ij}s_{ji}}$ and where $\kappa$ represents the thermal conductivity.

Let a small perturbation $\delta U=(\delta v_i,\delta\tau_{ij},\delta p,\delta T)$ be superposed on the set of homogeneous solutions $U=(v_i,\tau_{ij},p,T)$ of the system (4.1):

$$U\Rightarrow U+\delta U \qquad \text{with} \quad \delta U\ll U.$$

Homogeneous solutions evolution is supposed to be slower than perturbations (see also KERYVIN *et al.* [26]): the system is considered to be temporarily frozen. The perturbed system can thus be studied independently.

After linearization, it takes the form:

$$
\begin{aligned}
\delta\tau_{ij,j}-\rho_0\delta\dot{v}_i &= 0,\\
\rho_0C\delta\dot{T}-\kappa\delta T_{,kk}-(\delta J_2-\delta r)\dot{p}-(J_2-r)\delta\dot{p} &= 0,\\
\frac{1}{2}(\delta v_{i,j}+\delta v_{j,i})-\frac{3}{2}\delta\dot{p}\frac{s_{ij}}{J_2}-\frac{3}{2}\dot{p}\delta\left(\frac{s_{ij}}{J_2}\right) &= 0,\\
\delta\dot{p}-\delta\Lambda^p(\tau_{ij},p,T) &= 0.
\end{aligned}
\tag{4.2}
$$

Let the perturbation have a wave-like form:

$$\delta U=\overline{U}\exp\left(\varpi t+ik\underline{n}\,\underline{x}\right)=\overline{U}\exp[\varpi_R t]\exp\left[ik\left(ct+\underline{n}\,\underline{x}\right)\right] \tag{4.3}$$

where $\overline{U}$ represents the perturbation magnitude, $\varpi$ the wave pulsation, $k$ the wave number, $\underline{n}$ the wave vector, $\varpi_R$ and $\varpi_I$ respectively the real and imaginary parts of the wave pulsation $\varpi$, and $c=\varpi_I/k$ the wave velocity.

According to the right-hand term of (4.3), the case $\varpi_R=0$ points the transition between the stable and unstable states:

- if $\varpi_R>0$, the perturbation increases with time;
- if $\varpi_R<0$, the perturbation decreases with time.

The objective consists in looking for the conditions of the transition from the stable state to the unstable state by studying the sign of $\varpi_R$.

After injecting the perturbation (4.3) into the system (4.2), one obtains:

$$
\begin{aligned}
ikn_j\overline{\tau}_{ji}-\rho_0\varpi\overline{v}_i &= 0,\\
\left(\rho_0C\varpi+\kappa k^2+S^0\dot{p}\right)\overline{T}-\dot{p}\frac{3}{2}\frac{s_{ij}\overline{\tau}_{ji}}{J_2}+\left[Q^0\dot{p}-(J_2-r)\varpi\right]\overline{p} &= 0,\\
\frac{ik}{2}\left(n_j\overline{v}_i+n_i\overline{v}_j\right)-\frac{3}{2}\frac{s_{ij}}{J_2}\varpi\overline{p}-\dot{p}G_{ijkl}\overline{\tau}_{kl} &= 0,\\
(\varpi-B)\overline{p}-P_{ij}\overline{\tau}_{ji}-E\overline{T} &= 0,
\end{aligned}
\tag{4.4}
$$

with

$$Q^0 = \frac{\partial r}{\partial p}; \qquad S^0 = \frac{\partial r}{\partial T}; \qquad G_{ijkl} = \frac{3}{2}\frac{\partial\left(\frac{s_{ij}}{J_2}\right)}{\partial \tau_{kl}};$$
$$P_{ij} = \frac{\partial \Lambda^p}{\partial \tau_{ij}}; \qquad B = \frac{\partial \Lambda^p}{\partial p}; \qquad E = \frac{\partial \Lambda^p}{\partial T}$$

(see Appendix B for further details).

The system (4.4) can be written as:

$$[\mathcal{M}]\{\overline{U}\} = \{0\}. \tag{4.5}$$

The next step consists in finding the roots $\varpi$ from the determinant of the matrix $[\mathcal{M}]$. In the case of a thermo-viscoplastic behaviour, the determinant is a $4^{\text{th}}$ degree polynomial in $\varpi$. Solutions are not trivial and require the knowledge of the perturbation direction.

In the particular case of simple shear, where $v_1 \neq 0$ and $\tau_{12} \neq 0$, the perturbed system (4.4) takes the form:

$$\begin{aligned} ikn_2\overline{\tau}_{12} - \rho_0\varpi\overline{v}_1 &= 0, \\ \left(\rho_0 C\varpi + \kappa k^2 + S^0\dot{p}\right)\overline{T} - \sqrt{3}\dot{p}\overline{\tau}_{12} + \left[Q^0\dot{p} - \left(\sqrt{3}\tau_{12} - r\right)\varpi\right]\overline{p} &= 0, \\ ikn_2\overline{v}_1 - \sqrt{3}\varpi\overline{p} &= 0, \\ (\varpi - B)\overline{p} - \sqrt{3}\alpha\overline{\tau}_{12} - E\overline{T} &= 0, \end{aligned} \tag{4.6}$$

or otherwise

$$\begin{bmatrix} -\rho_0\varpi & ikn_2 & 0 & 0 \\ 0 & -\sqrt{3}\dot{p} & \left[Q^0\dot{p} - \left(\sqrt{3}\tau_{12} - r\right)\varpi\right] & \left(\rho_0 C\varpi + \kappa k^2 + S^0\dot{p}\right) \\ ikn_2 & 0 & -\sqrt{3}\varpi & 0 \\ 0 & -\sqrt{3}\alpha & (\varpi - B) & -E \end{bmatrix} \tag{4.7}$$
$$\times \begin{Bmatrix} \overline{v}_1 \\ \overline{\tau}_{12} \\ \overline{p} \\ \overline{T} \end{Bmatrix} = \begin{Bmatrix} 0 \\ 0 \\ 0 \\ 0 \end{Bmatrix}.$$

The system (4.7) can be written as:

$$[\mathcal{M}]\{\overline{U}\} = \{0\}. \tag{4.8}$$

The direction of the pertubation is obviously collinear with $x_2$ and the determinant of the matrix $[\mathcal{M}]$ is a $3^{\text{rd}}$ degree polynomial in $\varpi$:

$$\det[\mathcal{M}] = a_3\varpi^3 + a_2\varpi^2 + a_1\varpi^1 + a_0 \tag{4.9}$$

where

$$
\begin{aligned}
a_3 &= 3\rho_0^2 C\alpha, \\
a_2 &= \rho_0 \left[3\left(E + S^0\alpha\right)\dot{p} + k^2\left(3\kappa\alpha + C\right)\right], \\
a_1 &= k^2\left[\kappa k^2 + S^0\dot{p} - \rho_0 CB - E\left(\sqrt{3}\tau_{12} - r\right)\right], \\
a_0 &= k^2\left[\left(EQ^0 - BS^0\right)\dot{p} - \kappa k^2 B\right].
\end{aligned} \tag{4.10}
$$

Assuming adiabatic conditions ($\kappa = 0$), the coefficients (4.10) are reduced to:

$$
\begin{aligned}
a_3 &= 3\rho_0^2 C\alpha, \\
a_2 &= \rho_0 \left[3\left(E + S^0\alpha\right)\dot{p} + k^2 C\right], \\
a_1 &= k^2\left[S^0\dot{p} - \rho_0 CB - E\left(\sqrt{3}\tau_{12} - r\right)\right], \\
a_0 &= k^2\left(EQ^0 - BS^0\right)\dot{p},
\end{aligned} \tag{4.11}
$$

$$
\begin{aligned}
E + S^0\alpha &= -\alpha\frac{\partial R_0}{\partial T}, \\
EQ^0 - BS^0 &= -\alpha\frac{\partial R_0}{\partial T}Q^0,
\end{aligned} \tag{4.12}
$$

(see Appendix B for further details).

As stated previously, the idea is to delay the instability onset to approach the strong localization incipience. Adiabatic shear banding occurs as thermal softening overcomes the plastic hardening. In the constitutive model developed in Section 3, thermal softening is described through the partial derivatives of the hardening conjugate force $r\left(T; p, \widetilde{\mathbf{D}}\right)$ and of the internal stress $R_0\left(T; \widetilde{\mathbf{D}}\right)$ with respect to temperature. By neglecting the last contribution ($\partial R_0/\partial T = 0$) to thermal softening, the aforementioned delayed estimation (an "upper" bound for the instability onset) is reached without losing the mechanical consistency.

It is noteworthy that this simplification facilitates obtaining the analytical results. The expressions (4.12) become indeed zero, as also the coefficient $a_0$ in (4.11). The degree of the polynomial (4.9) is then equal to 2, and analytical solutions are obvious.

With the simplification $\partial R_0/\partial T = 0$ in the stability analysis, the coefficients (4.11) become:

$$
\begin{aligned}
a_3 &= 3\rho_0^2 C\alpha, \\
a_2 &= \rho_0 k^2 C, \\
a_1 &= k^2\left[S^0\dot{p} - \rho_0 CB - E\left(\sqrt{3}\tau_{12} - r\right)\right], \\
a_0 &= 0.
\end{aligned} \tag{4.13}
$$

As shown above, the determinant of the matrix $[\mathcal{M}]$ is a $2^{\text{nd}}$ degree polynomial in $\varpi$:

$$\det[\mathcal{M}] = a_3\varpi^2 + a_2\varpi + a_1 = 0. \tag{4.14}$$

The condition of instability may thus be written as:

$$\varpi > 0 \qquad \text{if and only if} \quad a_1 a_3 < 0.$$

The perturbation grows if and only if

$$3\rho_0^2 C\alpha k^2 \left[S^0\dot{p} - \rho_0 CB - E\left(\sqrt{3}\tau_{12} - r\right)\right] < 0, \tag{4.15}$$

or else, with the relations in Appendix B,

$$\frac{\partial r}{\partial p} < \frac{\left(\sqrt{3}\tau_{12} - r\right) + \dfrac{\dot{p}}{\alpha}}{\rho_0 C}\left(-\frac{\partial r}{\partial T}\right). \tag{4.16}$$

With $\dfrac{\dot{p}}{\alpha} = \dfrac{Y\dot{p}^{1/n}}{n}$, inequality (4.16) becomes:

$$\frac{\partial r}{\partial p} < \frac{\left(\sqrt{3}\tau_{12} - r\right) + \dfrac{Y\dot{p}^{1/n}}{n}}{\rho_0 C}\left(-\frac{\partial r}{\partial T}\right). \tag{4.17}$$

This condition of instability involves plastic hardening and thermal softening through the partial derivatives of the isotropic hardening conjugate force $r\,(T; p, \mathbf{D})$.

Consider another expression of inequality (4.16) as follows:

$$\mathcal{G}\left(\tau_{ij}, r, \dot{p}; \frac{\partial r}{\partial p}, \frac{\partial r}{\partial T}\right) = \sqrt{3 s_{ij} M_{ji} s_{kl} M_{lk}} - \left(r - \frac{Y\dot{p}^{1/n}}{n} + \rho_0 C \frac{\dfrac{\partial r}{\partial p}}{\left(-\dfrac{\partial r}{\partial T}\right)}\right) > 0. \tag{4.18}$$

Inequality (4.18) relates the resolved shear stress $\tau_{\text{res}} = s_{ij}M_{ji}$ to the isotropic conjugate force $r$, the strain rate-induced overstress $Y\dot{p}^{1/n}$, and the ratio of the plastic hardening $\partial r/\partial p$ to the thermal softening $\partial r/\partial T$.

In the present simplified analysis, the damage process is actually assumed to run as soon as $\mathcal{G}\left(\tau_{ij}, r, \dot{p}; \dfrac{\partial r}{\partial p}, \dfrac{\partial r}{\partial T}\right) = 0$. This latter condition must be interpreted as the auxiliary indicator for the damage process incipience leading to the

determination of the damage conjugate force threshold $k_{\text{inc}} = \text{Tr}\left(\widetilde{\mathbf{kN}}\right)_{\text{inc}}$ in the model of Section 3, see Eq. (3.36). Though a delay has been introduced in the instability onset, this condition is surely necessary but not sufficient, as shown in [24]. Further advanced studies involving the onset of strain localization in the presence of multiple mechanisms of inelastic deformation can be envisioned following the lines of the recent study by PETRYK [27]. The latter would necessitate adaptation to the rate-dependent constitutive framework.

It is noteworthy that the criterion (4.18) is obtained from an analysis based on the linear perturbation method, and not from an arbitrary, or purely phenomenological, damage incipience criterion.

## 5. Preliminary evaluation and comments on model capacities

The three-dimensional constitutive model developed in Sec. 3 is tested on a volume element (material point) loaded in simple shear in the context of adiabatic dynamic process. The time integration procedure is purely explicit and the time increment is imposed at the beginning of the analysis. The simple shear loading is applied via the velocity gradient $l_{12}$ (Fig. 6). The damage process (strong deformation localization) is supposed to occur inside the material through the development of a single shear band pattern of normal vector $\underline{n}$ collinear with the $\underline{x}_2$ axis (Fig. 5). The calculation of $k_{\text{inc}}$ is determined via the auxiliary method detailed in Sec. 4.

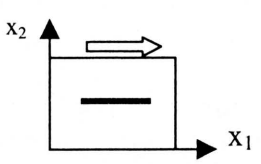


FIG. 5. Volume element containing a band.

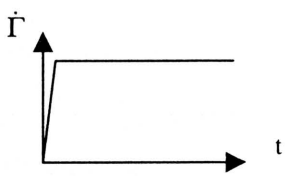


FIG. 6. Nominal shear strain rate history.

The nominal deformation gradient $\mathbf{F}$, the nominal velocity gradient $\mathbf{l}$, and the damage variable $\widetilde{\mathbf{D}}$ are given by:

$$[F] = \begin{bmatrix} 1 & \Gamma & 0 \\ 0 & 1 & 0 \\ 0 & 0 & 1 \end{bmatrix}, \quad [l] = \dot{\Gamma} \begin{bmatrix} 0 & 1 & 0 \\ 0 & 0 & 0 \\ 0 & 0 & 0 \end{bmatrix}, \quad [D] = d \begin{bmatrix} 0 & 0 & 0 \\ 0 & 1 & 0 \\ 0 & 0 & 0 \end{bmatrix},$$

where $\dot{\Gamma}$ represents the nominal shear strain rate, and $\Gamma$ the nominal shear strain.

In order to illustrate the model capabilities, experimental data by MARCHAND and DUFFY [5] have been chosen as general reference. The curve (Fig. 7)

they obtained from a high strain rate torsional test on a HY 100 steel tubular sample is usually used to illustrate adiabatic shear banding effects. This curve displays three consecutive stages: in the 1st stage, thermo-elastic/viscoplastic behaviour is stable; in the 2nd stage, a weak instability in flow appears; in the 3rd stage, the instability becomes strong and the deformation localizes through adiabatic shear bands. Model constants (Table 1) have been identified from these experimental data (Fig. 7). Consequently, the curve in Fig. 8 should not be considered as the one validating the model; it reproduces simply the experimental curve of Fig. 7. The discussion of model capabilities will be given below on the basis of specific additional correlations concerning the actual model, namely its response in terms of the state variables and their conjugate forces. Finally, by modifying the loading conditions given by [5], the beginning of validation will be considered (Figs. 22, 23).

**Table 1. Material constants of the constitutive model (Section 3).**

| $\rho_0$ (kg/m$^3$) | $C$ (J/kg·K) | $E$ (MPa) | $\nu$ | $\alpha$ (K$^{-1}$) | $a$ (MPa) | $b$ (MPa) |
|---|---|---|---|---|---|---|
| 7800 | 500 | 200e+3 | 0.33 | 1e−6 | 0 | 15e+3 |

| $R_i$ (MPa) | $R_{oo}$ (MPa) | $k$ | $\gamma(°C^{-1})$ | $d_1$ | $d_2$ | $\eta_2(MPa^{-2})(N=2)$ |
|---|---|---|---|---|---|---|
| 510 | 400 | 20 | 1.5e−3 | 0.05 | 0.05 | 0.01 |

| $Y$ (MPa·s$^{1/n}$) | $n$ | $Z$ (MPa·s$^{1/m}$) | $m$ |
|---|---|---|---|
| 100 | 10 | 10 | 2 |

Following simulations have been performed for $T_0 = 20°\text{C}$ and $\dot{\Gamma} = 1600\ \text{s}^{-1}$. The value of nominal shear strain at the damage incipience (strong deformation localization onset) is close to 39%.

Numerical strain components have been drawn versus the nominal shear strain $\Gamma$ in Figs. 9 to 11. Strains have been obtained by integration from the corresponding expressions giving strain rates as follows:

$$(5.1)\qquad \begin{aligned} \dot{v}_{ij} &= d_{ij} + W_{ik}v_{kj} - v_{ip}W_{pj} \\ v_{ij}^{n+1} &= v_{ij}^{n} + \dot{v}_{ij}^{n+1}\cdot\Delta t \end{aligned} \qquad \text{where} \qquad \begin{aligned} v_{ij} &= \left(e_{ij}, e_{ij}^{e}, e_{ij}^{p}, e_{ij}^{d}\right), \\ d_{ij} &= \left(d_{ij}, d_{ij}^{e}, d_{ij}^{p}, d_{ij}^{d}\right). \end{aligned}$$

After the onset of damage, damage-related strain contribution increases while both elastic strain and plastic "regular" rate decrease: as the deformation concentrates more and more inside the bands, the mechanism of damage replaces progressively the mechanism of "regular" plasticity.

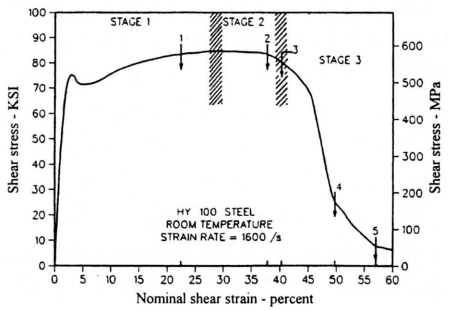


FIG. 7. Experimental stress-strain curve showing behaviour softening by ASB (after MARCHAND and DUFFY, [5]).

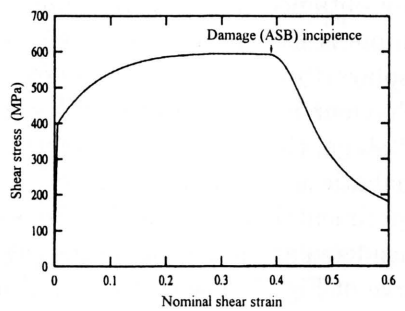


FIG. 8. Shear stress $\tau_{12}$ vs. nominal shear strain $\Gamma$ reproduced by the 3D model.

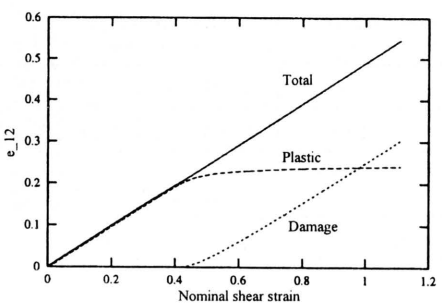


FIG. 9. Strain $e_{12}$ vs. nominal shear strain $\Gamma$.

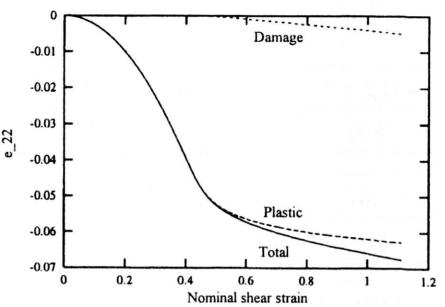


FIG. 10. Strain $e_{22}$ vs. nominal shear strain $\Gamma$.

Numerical spin components have been drawn versus the nominal shear strain $\Gamma$ in Fig. 12. According to (3.45), the rotation rate $\mathbf{W}$ represents, in the absence of damage, the spin $\boldsymbol{\omega}$ obtained from the anti-symmetric part of the velocity gradient $\mathbf{l}$. In this case, the objective derivative is simply the Zaremba-Jaumann derivative. After the onset of damage, Fig. 12 shows how the increase of damage-induced spin $\boldsymbol{\omega}^{\mathbf{d}}$ leads to the decrease of the rotation rate $\mathbf{W}$.

Total strain components have been drawn versus the nominal shear strain $\Gamma$ in Fig. 13. After a value of nominal shear strain $\Gamma$ close to 10%, strain components $e_{11}$ and $e_{22}$ increase and become significant compared with the strain $e_{12}$. This induces a change of the ratio $e_{12}/\Gamma$ which is initially equal to $1/2$. Finite rotation-related terms which appear in the time derivative $(5.1)_1$ are directly responsible for the existence of both strain components $e_{11}$ and $e_{22}$. In the small deformation framework, these strain components would be zero because $(5.1)_1$ should be reduced to $v_{ij} = d_{ij}$. This remark concerns also time derivative of stress.

"Regular" temperature has been drawn versus the nominal shear strain $\Gamma$ in Fig. 14. "Regular" temperature increases indeed until the damage onset. During the damage process, "regular" heating contribution decreases while "singular" heating contribution increases (see (3.32)) in relation to the damage variable growth.

Components of the thermo-elastic Kirchhoff stress tensor $\tau$ (called $S\_ij$) have been drawn versus the nominal shear strain $\Gamma$ in Fig. 15. The existence of stress components different from $\tau_{12}$ is a direct consequence of the finite deformation framework (see the remarks on strain derivatives). The various stress contributions to the generalized 2nd invariant $\hat{J}_2^s$ (called $J_2$) have been detailed in Fig. 16. It is noteworthy that, while the shear stress $\tau_{12}$ decreases strongly, the isotropic hardening conjugate force $r$ remains significant. This preserves a certain strength of the material outside the bands.
The first invariant (density $d$) of the damage variable $\mathbf{D}$ has been drawn versus the nominal shear strain $\Gamma$ in Fig. 17.

At the end of the calculations, the value of $d$ is about 3. Interpretation of this result needs returning to the definition (2.2) of the density d of the damage variable $\mathbf{D}$:

$$d = d(T^*, ...).$$

In the case of simple shear, neglecting second order terms (resulting from complete time integration (5.1)), the thermo-elastic shear stress $(3.26)_1$ is approximately:

$$\tau_{12} = 2\mu e_{12}^e - 2be_{12}^e\widetilde{D}_{22} = 2\left(\mu - b\widetilde{D}_{22}\right)e_{12}^e \tag{5.2}$$

where

$$\widetilde{D}_{22} = d\widetilde{n}_2\widetilde{n}_2, \qquad \widetilde{n} = (0,1,0). \tag{5.3}$$

According to (5.2) and (5.3), with the notation employed in (3.30), one can write:

$$C_{1212} = \mu - bd \tag{5.4}$$

where $C_{1212}$ represents the current "global" shear modulus and $\mu$ is the initial shear modulus.

As shown in Fig. 18 below, the shear modulus can be approximated by a 2nd degree polynomial in temperature, in the interval [300 K, 1000 K]:

$$\mu(T) = \mu(0) - c_1T - c_2T^2 \qquad \text{with} \quad \begin{cases} c_1 = 8.1e-3 \text{ GPa/K}, \\ c_2 = 2e-5 \text{ GPa/K}^2. \end{cases} \tag{5.5}$$

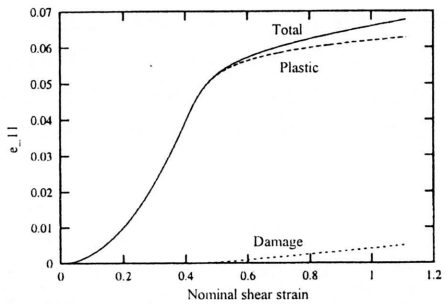


FIG. 11. Strain $e_{11}$ vs. nominal shear strain $\Gamma$.

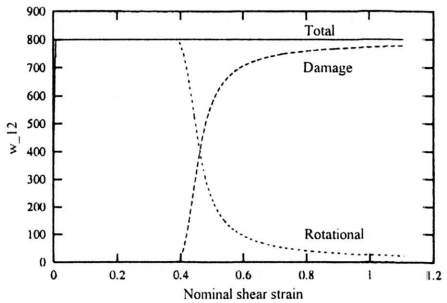


FIG. 12. Spin $w_{12}$ vs. nominal shear strain $\Gamma$.

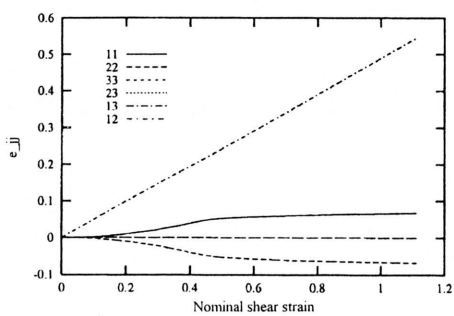


FIG. 13. Strains $e_{ij}$ vs. nominal shear strain $\Gamma$.

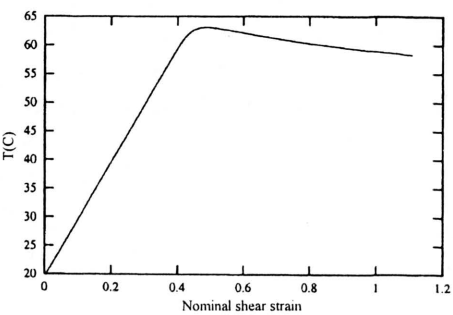


FIG. 14. "Regular" temperature vs. nominal shear strain $\Gamma$.

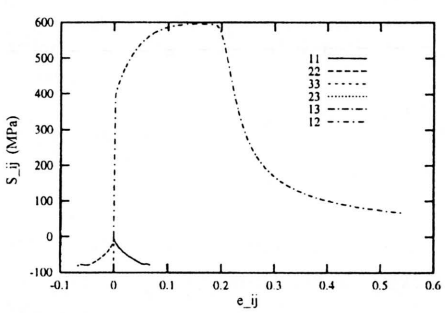


FIG. 15. Stress vs. nominal shear strain $\Gamma$.

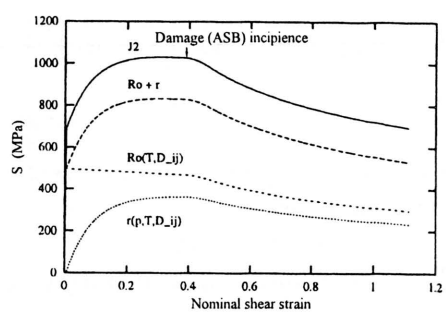


FIG. 16. $\hat{J}_2^s$ contributions vs. shear strain $\Gamma$.

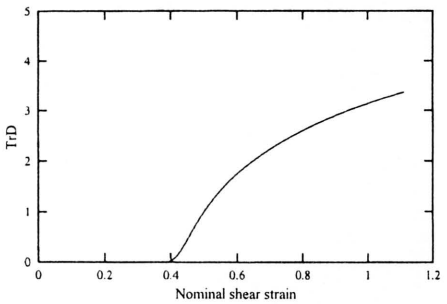


FIG. 17. Damage density vs. nominal shear strain $\Gamma$.

Fluctuations in shear modulus at low temperature (from 300 K to 400 K, which bound the range of "regular" temperature before the onset of damage) are weak, what justifies that the constitutive model supposes independence of the shear modulus $\mu$ from temperature in the elastic potential (3.15). On the other hand, at high temperature, especially inside the bands, the shear modulus is strongly affected. As the deformation is accommodated by ASB at advanced stage of localization, the current "global" shear modulus is close to the shear modulus of the band material.

Combining relations (5.4) from the present model with (5.5) yields:

$$\text{for } T > T_0^* \qquad C_{1212} = \mu(T^*) = \mu(0) - c_1 T^* - c_2 T^{*2} = \mu(T_0^*) - bd(T^*). \tag{5.6}$$

Rearranging (5.6) gives the following expression for $d(T^*)$:

$$d(T^*) = \frac{\mu(T_0^*) - \mu(0) + c_1 T^* + c_2 T^{*2}}{b}, \tag{5.7}$$

which verifies $d_{\min} = d(T_0^*) = 0$.

As a result of highly overestimating evaluation of an upper bound for $d = d(T^*)$, we can state first that temperature inside the band is bounded by the

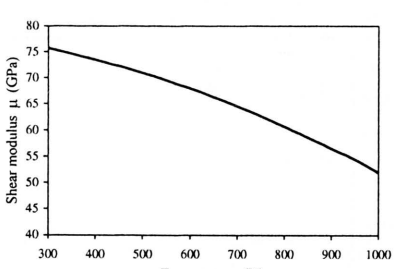


FIG. 18. Shear modulus $\mu$ vs. temperature for a hard steel (after JUANICOTENA [28] with $\mu(0) = 80$ GPa).

melting point. Consequently, the shear modulus is bounded by its value at the melting temperature. Extrapolating relation (5.5) to the melting temperature, the expression (5.7) gives the upper bound $d_{\max}$ of density $d$ as:

$$d_{\max} = d(T_m) = \frac{\mu(T_0^*) - \mu(0) + c_1 T_m + c_2 T_m^{*2}}{b}. \tag{5.8}$$

If $\mu(T_m) \approx 0$, the upper bound $d_{\max}$ can be crudely approximated from (5.8) by:

$$d_{\max} \approx \frac{\mu}{b}. \tag{5.9}$$

The value of the material constant $b$, related to elastic energy degradation through the degradation of the shear stiffness produced by adiabatic shear banding, governs the upper bound $d_{\max}$. In the present numerical example, the value of $b$ is chosen as 15 GPa (Table 1), which gives an upper bound for $d_{\max}$ close to 5. In the foregoing case (Fig. 17), the value close to 3 attained for nominal shear strain of about 1.2 is well below this limit. If prolonged further, the curve in Fig. 17 would ultimately approach (but never attain) the upper bound limit. Evolution of the current "global" shear modulus $C_{1212}$ versus the nominal shear strain $\Gamma$ is reported in Fig. 19.

In a tentative conclusion to this evaluation, it is interesting to note that when $b \to \mu$, then, according to (5.9), the interval of $d(T^*)$ is $[0, 1]$, and consequently, according to (5.4), the interval of $C_{1212}$ is $[\mu, 0]$. In that interval, $C_{1212}$ takes the values $\mu(1 - d(T^*))$ which can be approximated, following (5.7) and assuming independence of the shear modulus from temperature before damage incipience, by $\mu(0) - c_1 T^* - c_2 T^{*2}$. The shear stiffness of the representative volume becomes a function of the "singular" temperature only (with no $b$ explicitly intervening). Fluctuations in "singular" temperature inside the band cluster are thus directly and exclusively responsible for fluctuations in the shear stiffness of the representative volume. This limiting case can be further explored in the fu-

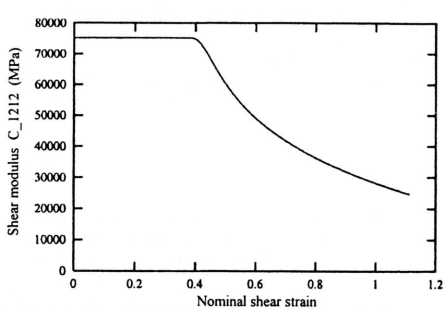


FIG. 19. Shear modulus $C_{1212}$ vs. nominal shear strain $\Gamma$.

ture, especially in the context of mesh sensitivity control when performing finite element numerical calculations.

The upper bound of $d(T^*)$ being related to the value of shear degradation constant $b$ (dependent on particular material) may represent some inconvenience in practical applications. Normalizing definitely the function $d(T^*)$ by fixing its maximum to, say e.g. 1, necessitates some technical modifications of the preceding equations (this will obviously shift in parallel the actual limit value of $d_{\max} = 1$ for $b \to \mu$). This subject will not be analysed here.

The components of the damage force tensor $\widetilde{\mathbf{k}}$ (called $k\_ij$) have been drawn versus the 1st invariant (density) of the damage variable in Fig. 20 and versus the nominal shear strain $\Gamma$ in Fig. 21. The damage conjugate force increases with the nominal shear strain. At the onset of damage, the component $\widetilde{k}_{22}$ diverges from $\widetilde{k}_{11}$ and $\widetilde{k}_{33}$ to increase more strongly in the damage process.

Different loading conditions have been imposed in shear to test the response of the model. Following effects have been illustrated in Figs. 22 and 23:

- nominal shear strain rate $\dot{\Gamma}$ effect on stress-nominal strain response;
- initial temperature $T_0$ effect on stress-nominal strain response.

Figure 22 shows that instability appears earlier when the nominal shear strain rate is higher. This agrees with the experimental investigations. Concurrently the influence of the nominal shear strain rate on stress increase is higher after the onset of damage.

Figure 23 shows that instability appears earlier when the initial temperature is lower. Numerical values of nominal shear strain $\Gamma$ at the onset of localization do not agree exactly with experimental values obtained in [5]. The influence of the nominal shear strain rate on stress is higher before the onset of damage.

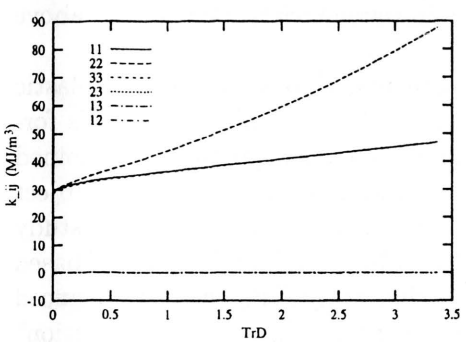


FIG. 20. Damage force $\widetilde{\mathbf{k}}$ vs. damage variable density $d$.

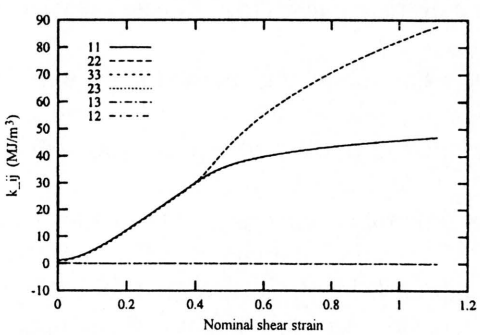


FIG. 21. Damage force $\widetilde{\mathbf{k}}$ vs. nominal shear strain $\Gamma$.

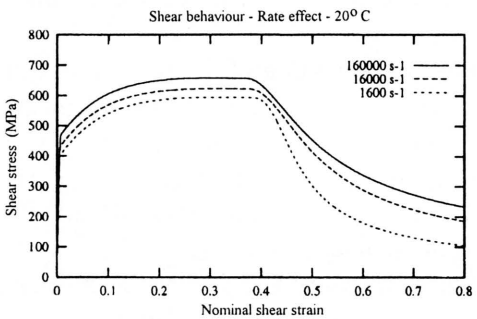


FIG. 22. Shear stress vs. nominal shear strain $\Gamma$, $T_0 = 20°$ C.

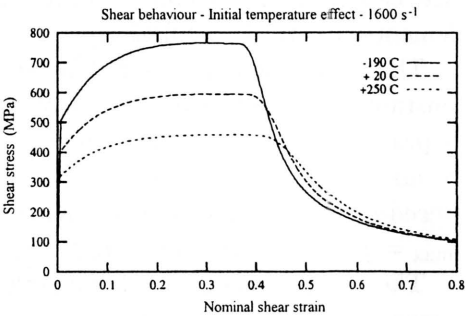


FIG. 23. Shear stress vs. nominal shear strain $\Gamma$, $\dot{\Gamma} = 1600\ \mathrm{s}^{-1}$.

## 6. Concluding remarks and perspectives

An elastic/viscoplastic constitutive model has been elaborated involving damage and damage-induced anisotropy produced by adiabatic shear banding. The latter deterioration mechanism has been captured through a second-order tensorial damage internal variable whose evolution is considered as rate-dependent (viscous) in some formal analogy to the plastic flow evolution.

As pointed out by PERZYNA *et al.* [11, 12], rate dependency favours maintaining ellipticity of the equations governing the evolution problem related to the class of constitutive models including the present one. The viscosity-related regularizing influence of the viscoplasticity and damage respective relaxation factors $Y$ and $Z$ (together with the exponents $n$ and $m$; see Eqs. (3.39)–(3.40)) allows to overcome local instabilities, as it is shown in the numerical simulations above (Sect. 5).

The modelling methodology put forward herein in the finite elastic-plastic strain Eulerian framework has had to face the difficulties inherent for this formulation to cope with anisotropy effects and objectivity requirements combined [15]. As there is no clear consensus of the scientific community on this subject (while some convergent methodologies can be noticed, see e.g. LUBARDA's study [17] including damage and EKH and RUNESSON [16]), the Mandel-Sidoroff based approach has been favoured and adapted in this study. The analogy advanced here between an adiabatic shear band (ASB) cluster and a "super-dislocation" leads to a fairly simple evaluation of the damage-induced spin. The objective rotational derivatives can thus be operational within the model framework. By combining these specific factors, relevant to kinematics and anisotropy hypotheses, with thermodynamic postulates (existence of the free energy and dissipa-

tion potentials, and their consequences), a coherent model could be formulated. Some simplifying assumptions, regarding notably the strain hardening description and small elastic strain, have been made. The assumption of a single damage-plasticity yield function allows to express the strong coupling between the dissipative mechanisms at stake.

Constraints relative to consistent formulation of discretized boundary value problem and to relevant numerical implementation of the model have constituted a significant guideline to the formulation presented. Those aspects will be presented in details in forthcoming papers. Another question concerns the number and nature of material constants involved in the formulation presented. A compromise has been searched between conceptual pertinency of the constitutive model vs. complexity of mesomechanical and metallurgical phenomena and the tractability of the formalism advanced when applied to high velocity impact and penetration engineering problems. Those applications are currently under way.

## Appendix A

$$C_{ijkl} = \rho_0 \frac{\partial^2 \psi}{\partial e^e_{ij} \partial e^e_{kl}} = \lambda \delta_{ij}\delta_{kl} + \mu(\delta_{ik}\delta_{jl} + \delta_{il}\delta_{jk}) - a\left(\delta_{ij}\widetilde{D}_{kl} + \widetilde{D}_{ij}\delta_{kl}\right) - b\left[\delta_{ik}\widetilde{D}_{jl} + \delta_{il}\widetilde{D}_{jk} + \widetilde{D}_{ik}\delta_{jl} + \widetilde{D}_{il}\delta_{jk}\right],$$

$$E_{ijkl} = \rho_0 \frac{\partial^2 \psi}{\partial e^e_{ij} \partial \widetilde{D}_{kl}} = -a\left[\delta_{ij}e^e_{kl} + \frac{e^e_{pp}}{2}(\delta_{ik}\delta_{jl} + \delta_{il}\delta_{jk})\right] - b\left[e^e_{ik}\delta_{jl} + e^e_{il}\delta_{jk} + \delta_{ik}e^e_{jl} + \delta_{il}e^e_{jk}\right],$$

$$J_{ij} = \rho_0 \frac{\partial^2 \psi}{\partial e^e_{ij} \partial T} = -\alpha K \delta_{ij};$$

$$Q = \rho_0 \frac{\partial^2 \psi}{\partial p^2} = kR_\infty \exp(-kp) \exp(-\gamma T) \exp\left(-d_1 \widetilde{D}_{kk} - \frac{d_2}{2}\widetilde{D}_{kl}\widetilde{D}_{lk}\right),$$

$$A_{ij} = \rho_0 \frac{\partial^2 \psi}{\partial p \partial \widetilde{D}_{ij}} = -R_\infty [1 - \exp(-kp)] \exp(-\gamma T) \cdot \exp\left(-d_1 \widetilde{D}_{kk} - \frac{d_2}{2}\widetilde{D}_{kl}\widetilde{D}_{lk}\right)\left[d_1 \delta_{ij} + d_2 \widetilde{D}_{ij}\right],$$

$$S = \rho_0 \frac{\partial^2 \psi}{\partial p \partial T} = -\gamma R_\infty [1 - \exp(-kp)] \exp(-\gamma T) \exp\left(-d_1 \widetilde{D}_{kk} - \frac{d_2}{2}\widetilde{D}_{kl}\widetilde{D}_{lk}\right);$$

$$L_{ijkl} = \rho_0 \frac{\partial^2 \psi}{\partial \widetilde{D}_{ij} \partial \widetilde{D}_{kl}}$$
$$= +R_\infty \left[ p + \frac{1}{k} \exp(-kp) \right] \exp(-\gamma T) \exp\left( -d_1 \widetilde{D}_{pp} - \frac{d_2}{2} \widetilde{D}_{mn} \widetilde{D}_{nm} \right)$$
$$\left\{ \left[ d_1 \delta_{ij} + d_2 \widetilde{D}_{ij} \right] \left[ d_1 \delta_{kl} + d_2 \widetilde{D}_{kl} \right] - \frac{d_2}{2} \left[ \delta_{ik} \delta_{jl} + \delta_{il} \delta_{jk} \right] \right\},$$

$$V_{ij} = \rho \frac{\partial^2 \psi}{\partial \widetilde{D}_{ij} \partial T} = \gamma R_\infty \left[ p + \frac{1}{k} \exp(-kp) \right]$$
$$\cdot \exp(-\gamma T) \exp\left( -d_1 \widetilde{D}_{kk} - d_2 \widetilde{D}_{kl} \widetilde{D}_{lk} \right) \left[ d_1 \delta_{ij} + d_2 \widetilde{D}_{ij} \right],$$

$$X = \rho_0 \frac{\partial^2 \psi}{\partial T^2}$$
$$= -\frac{\rho C}{T_0} + \gamma^2 R_\infty \left[ p + \frac{1}{k} \exp(-kp) \right] \exp(-\gamma T) \exp\left( -d_1 \widetilde{D}_{kk} - d_2 \widetilde{D}_{kl} \widetilde{D}_{lk} \right).$$

## Appendix B

$$Q^0 = \frac{\partial r}{\partial p} = k R_\infty \exp(-kp) \exp(-\gamma T),$$
$$S^0 = \frac{\partial r}{\partial T} = -\gamma R_\infty \left[ 1 - \exp(-kp) \right] \exp(-\gamma T),$$
$$G_{ijkl} = \frac{3}{2} \frac{\partial \left( \frac{s_{ij}}{J_2} \right)}{\partial \tau_{kl}} = \frac{3}{2 J_2} \left[ I_{ijkl} - \frac{1}{3} \delta_{ij} \delta_{kl} - \frac{3}{2} \frac{s_{ij} s_{kl}}{J_2^2} \right];$$
$$P_{ij} = \frac{\partial \Lambda^p}{\partial \tau_{ij}} = \frac{\partial \Lambda^p}{\partial \mathcal{F}} \frac{\partial \mathcal{F}}{\partial \tau_{ij}} = \alpha K_{ij} = \frac{3}{2} \alpha \frac{s_{ij}}{J_2},$$
$$B = \frac{\partial \Lambda^p}{\partial p} = \frac{\partial \Lambda^p}{\partial \mathcal{F}} \frac{\partial \mathcal{F}}{\partial p} = -\alpha \frac{\partial r}{\partial p} = -\alpha Q^0,$$
$$E = \frac{\partial \Lambda^p}{\partial T} = \frac{\partial \Lambda^p}{\partial \mathcal{F}} \frac{\partial \mathcal{F}}{\partial T} = -\alpha \left( \frac{\partial R_0}{\partial T} + \frac{\partial r}{\partial T} \right) = -\alpha \left( \frac{\partial R_0}{\partial T} + S^0 \right);$$

$$\alpha = \frac{\partial \Lambda^p}{\partial \mathcal{F}} = n \frac{\dot{p}^{1 - \frac{1}{n}}}{Y}$$

$$EQ^0 = \frac{\partial \Lambda^p}{\partial T}\frac{\partial r}{\partial p} = -\alpha\left(\frac{\partial R_0}{\partial T} + S^0\right)Q^0$$

$$BS^0 = \frac{\partial \Lambda^p}{\partial p}\frac{\partial r}{\partial T} = -\alpha Q^0 S^0$$

$$\text{then} \quad \begin{cases} E + S^0\alpha = -\alpha\dfrac{\partial R_0}{\partial T} \\ EQ^0 - BS^0 = -\alpha\dfrac{\partial R_0}{\partial T}Q^0. \end{cases}$$

## References


1. R. L. WOODWARD, *Material failure at high strain rates*, [in:] *High velocity impact dynamics*, J.A. ZUKAS [Ed.], John Wiley & Sons, 65–125 1990.
2. S. NEMAT-NASSER, Y-F. LI and J. B. ISAACS, *Experimental/computational evaluation of flow stress at high strain rates with applications to adiabatic shear banding*, Mech. Mat., **17**, 111–134, 1994.
3. Y.L. BAI, *Thermo-plastic instability in simple shear*, J. Mech. Phys. Solids, **30**, 4, 195–207, 1982.
4. T. WRIGHT and R. BATRA, *The initiation and growth of adiabatic shear bands*, Int. J. Plasticity, **1**, 205–212, 1985.
5. A. MARCHAND and J. DUFFY, *An experimental study of the formation process of adiabatic shear bands in a structural steel*, J. Mech. Phys. Solids, **36**, 3, 251–283, 1988.
6. S. MERCIER and A. MOLINARI, *Steady-state shear band propagation under dyanmic conditions*, J. Mech. Phys. Solids, **46**, 8, 1463–1495, 1998.
7. A. MOLINARI, *Collective behavior and spacing of adiabatic shear bands*, J. Mech. Phys. Solids, **45**, 9, 1551–1575, 1997.
8. D.E. GRADY, *Dissipation in adiabatic shear bands*, Mech. Mat., **17**, 289–293, 1994.
9. R.B. PĘCHERSKI, *Macroscopic effects of micro-shear banding in plasticity of metals*, Acta Mech., **131**, 203–224, 1998.
10. P. PERZYNA, *Influence of anisotropic effects on the micro-damage process in dissipative solids*, [in:] *Yielding, Damage, and Failure of Anisotropic Solids*, J.P. BOEHLER [Ed.], Mech. Engng Pub., 483–507, 1990.
11. T. ŁODYGOWSKI and P. PERZYNA, *Localized fracture in inelastic polycrystalline solids under dynamic loading processes*, Int. J. Damage Mech., **6**, 364–407, 1997.
12. W. DORNOWSKI and P. PERZYNA, *Localization phenomena in thermo-viscoplastic flow processes under cyclic dynamic loadings*, Comp. Assist. Mech. Engng Sci., **7**, 117–160, 2000.
13. A. DRAGON, D. HALM and T. DÉSOYER, *Anisotropic damage in quasi-brittle solids: modelling, computational issues and applications*, Computer Meth. Appl. Mech. Engng, **183**, 331–352, 2000.
14. J. MANDEL, *Equations constitutives et directeurs dans les milieux plastiques et viscoplastiques*, Int. J. Solids Structures, **9**, 725–740, 1973.
15. F. SIDOROFF and A. DOGUI, *Some issues about anisotropic elastic-plastic models at finite strain*, Int. J. Solids Structures, **38**, 9569–9578, 2001.
16. M. EKH and K. RUNESSON, *Modeling and numerical issues in hyperelasto-plasticity with anisotropy*, Int. J. Solids Structures, **38**, 9461–9478, 2001.

17. V. A. LUBARDA, *An analysis of large-strain damage elastoplasticity*, Int. J. Solids Structures, **31**, 2951–2964, 1994.
18. Y. F. DAFALIAS, *A missing link in the macroscopic constitutive formulation of large plastic deformations*, [in:] *Plasticity Today*, A. SAWCZUK and G. BIANCHI [Eds.], Elsevier, 1983.
19. J. P. BOEHLER, *Lois de comportement anisotrope des milieux continus*, J. Mécanique, **17**, 153–190, 1978.
20. A. DOGUI and F. SIDOROFF, *Quelques remarques sur la plasticité anisotrope en grandes déformations*, C. R. Acad. Sc. Paris, **299**, Série II, n°18, 1225–1228, 1984.
21. P. PERZYNA, *Fundamental problems in viscoplasticity*, Rec. Adv. Appl. Mech., **9**, 243–377, Academic Press, New York 1966.
22. J. MANDEL, *Relations de comportement pour un solide élastoplastique anisotrope en transformation finie*, [in:] *Comportement plastique des solides anisotropes*, Colloque international n°319 du CNRS, Villard-de-Lans, pp. 197–210, 1981.
23. R. J. CLIFTON, J. DUFFY, K. A. HARTLEY and T. G. SHAWKI, *On critical conditions for shear band formation at high strain rates*, Scripta Met., **18**, 443–448, 1984.
24. A. MOLINARI, *Instabilité thermoviscoplastique en cisaillement simple*, J. Méca. Théorique et Appliquée, **4**, 659–684, 1985.
25. T.G. SHAWKI and R. J. CLIFTON, *Shear band formation in thermal viscoplastic materials*, Mech. of Materials, **8**, 13–43, 1989.
26. V. KERYVIN, T. DÉSOYER and J.L. HANUS, *Localisation de la déformation sous sollicitations lentes: une approche dynamique*, C. R. Acad. Sc. Paris, **328**, Série IIb, 727–732, 2000.
27. H. PETRYK, *General conditions for uniqueness in materials with multiple mechanisms of inelastic deformation*, J. Mech. Phys. Solids, **48**, 367–396, 2000.
28. A. JUANICOTENA, *Etude théorique et expérimentale du comportement viscoplastique des matériaux aux grandes déformations et grandes vitesses de déformation; Application à l'acier Mars 190 et au tantale*, PhD Thesis, Université de Metz, 1998.

*Received July 26, 2002.*